International Journal of Nanomedicine

Dovepress
open access to scientific and medical research

Open Access Full Text Article

REVIEW

Recent Advances for Dynamic-Based Therapy of Atherosclerosis

Guanghao Wu[1,*], Guanye Yu[2,*], Meiling Zheng[3,*], Wenhui Peng[2], Lei Li[4]

[1]School of Materials Science and Engineering, Beijing Institute of Technology, Beijing, 100081, People's Republic of China; [2]Department of Cardiology, Shanghai Tenth People's Hospital, Tongji University, School of Medicine, Shanghai, 200072, People's Republic of China; [3]Dongzhimen Hospital Beijing University of Chinese Medicine, Beijing, 101121, People's Republic of China; [4]National Clinical Research Center for Obstetric & Gynecologic Diseases, Department of Obstetrics and Gynecology, Peking Union Medical College Hospital, Chinese Academy of Medical Sciences & Peking Union Medical College, Beijing, 100730, People's Republic of China

*These authors contributed equally to this work

Correspondence: Lei Li, Department of Obstetrics and Gynecology, Peking Union Medical College Hospital, Chinese Academy of Medical Sciences & Peking Union Medical College, No. 1 Shuai Fu Yuan, Eastern District, Beijing, 100730, People's Republic of China, Tel +8613426328126, Fax +86 10 69158100, Email lilei64@pumch.cn; Guanghao Wu, School of Materials Science and Engineering, Beijing Institute of Technology, Beijing, 100081, People's Republic of China, Email bitwgh@126.com

Abstract: Atherosclerosis (AS) is a chronic inflammatory disease, which may lead to high morbidity and mortality. Currently, the clinical treatment strategy for AS is administering drugs and performing surgery. However, advanced therapy strategies are urgently required because of the deficient therapeutic effects of current managements. Increased number of energy conversion-based organic or inorganic materials has been used in cancer and other major disease treatments, bringing hope to patients with the development of nanomedicine and materials. These treatment strategies employ specific nanomaterials with specific own physiochemical properties (external stimuli: light or ultrasound) to promote foam cell apoptosis and cholesterol efflux. Based on the pathological characteristics of vulnerable plaques, energy conversion-based nano-therapy has attracted increasing attention in the field of anti-atherosclerosis. Therefore, this review focuses on recent advances in energy conversion-based treatments. In addition to summarizing the therapeutic effects of various techniques, the regulated pathological processes are highlighted. Finally, the challenges and prospects for further development of dynamic treatment for AS are discussed.

Keywords: atherosclerosis, nanomaterial, physiochemical, reactive oxygen species, energy conversion, therapy

Introduction

Cardiovascular disorders are the leading causes of morbidity and mortality worldwide. According to the latest report by the World Health Organization (WHO), approximately 32% of deaths are due to cardiovascular diseases (CVDs).[1] CVDs are a group of disorders of the heart and blood vessels. Approximately 45.1% of these cardiovascular disease-related deaths were caused by coronary artery disease. Atherosclerosis (AS) is a chronic inflammatory vascular disease. Smoking, alcoholism, high-diet, lack of exercise, and genetic predisposition are important factors in the development of AS. These factors increase blood lipid concentration and lipid deposits in vessel wall would lead to formation of atherosclerotic plaque and gradually induce stenosis and obstruction of blood flow. Rupture of atherosclerotic plaque produces lesions that result in acute myocardial infarction, sudden cardiac death, or other severe outcomes.[2,3]

Until now, clinical treatments for AS focused on drugs and surgery; angioplasty and bypass grafting are the two main surgical interventions.[4,5] However, surgery is invasive and may induce thrombosis in the endarterectomized segment, which may increase the risk of thrombosis, bleeding, and restenosis. Statins, which are an important drug intervention, are thought to be important in the prevention of AS. These drugs could not only reduce cholesterol but also alleviate pro-inflammatory cytokine effects. Besides statins, some other drugs, such as proprotein convertase subtilisin/kexin type 9 inhibitors (Alirocumab and Evolocumab), could enhance low-density lipoprotein (LDL) degradation and promote lower cholesterol levels.[6] In addition, certain immunosuppressants (methotrexate and rapamycin) show a clear and promising

Received: 26 December 2022
Accepted: 6 May 2023
Published: 13 July 2023

impact in reducing atherosclerotic plaque sizes. However, there are still some limitations in terms of stability, targeting efficacy, toxicity, and production. Currently, the combination of nanotechnology and AS offers hope for the treatment of these diseases. Compared with traditional nano-therapies, energy conversion-based nano-therapy can not only leverage external energy for proapoptotic effects on the foam cells of vulnerable plaques but also allow for minimal dosing to achieve therapeutic effects and migrated side-effects. Previous studies have summarized the use of nanomedicine in the treatment and imaging of atherosclerotic plaques. To the best of our knowledge, there is no comprehensive and systematic review of nano-dynamic treatment strategies for AS. In this review, we explored and illustrated the mechanism of atherosclerotic plaque formation and highlighted the current characteristics of phototherapy—both photothermal therapy (PTT) and photodynamic therapy (PDT—and sonodynamic therapy (SDT)) for AS treatment (Figure 1).

The Pathogenesis of Atherosclerotic Plaques

The formation of atherosclerotic plaque is a continuous and complicated process with early and advanced stages. A schematic diagram of the stages of atherosclerosis formation is shown in Figure 2. At early stage, toxic substances such as nicotine, high level of cholesterol and glucose in blood, which are brought by maladaptive lifestyle, would damage the balance of microenvironment, and hemodynamic disorder like hypertension further aggravates the situation, further damages endothelium.[7–9] Maladaptive living and eating habits could lead to endothelial dysfunction. Endothelial dysfunction is a critical pathophysiological element in AS, inducing greater penetration of macromolecules such as lipoproteins, and increasing production of chemotactic molecules (ICAM-1, VCAM-1, and P-selectin). Next, monocytes differentiate into macrophages and transform into foam cells by ingesting oxidized low-density lipoprotein (ox-LDL) via

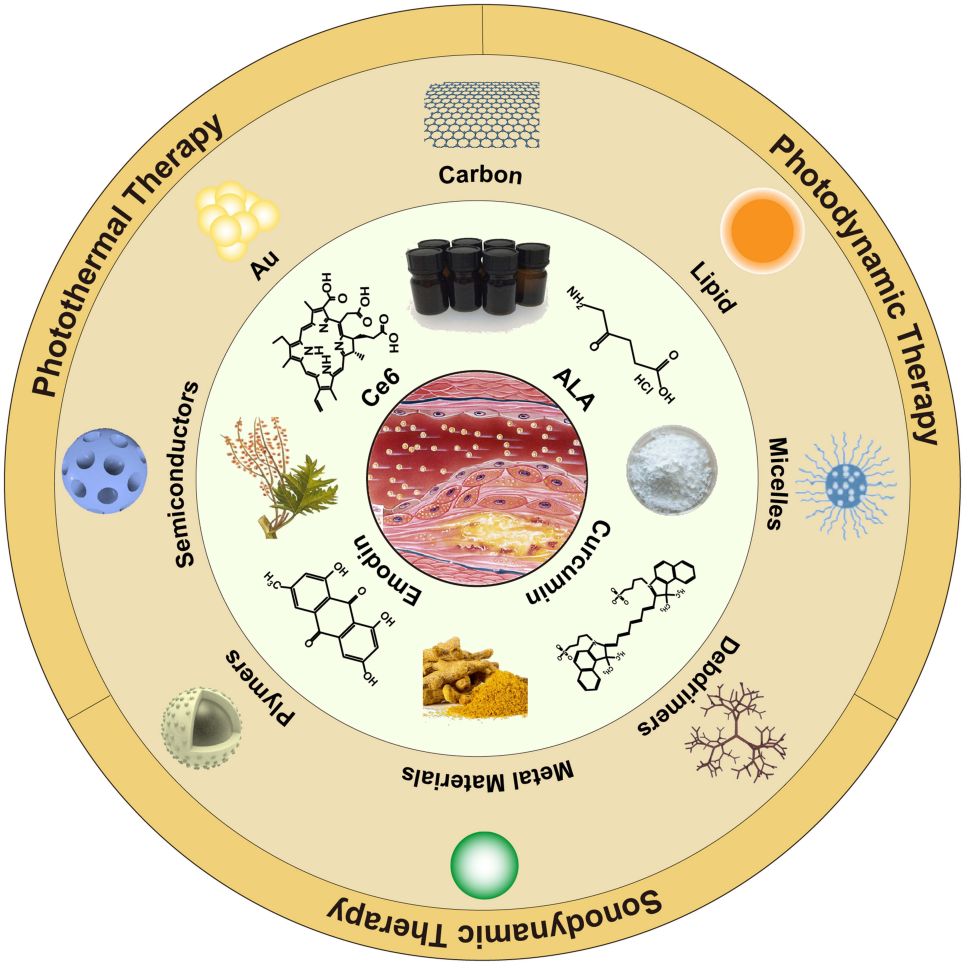

Figure 1 Schematics of nanomaterials and conventional agents for energy conversion-based therapies for atherosclerosis.

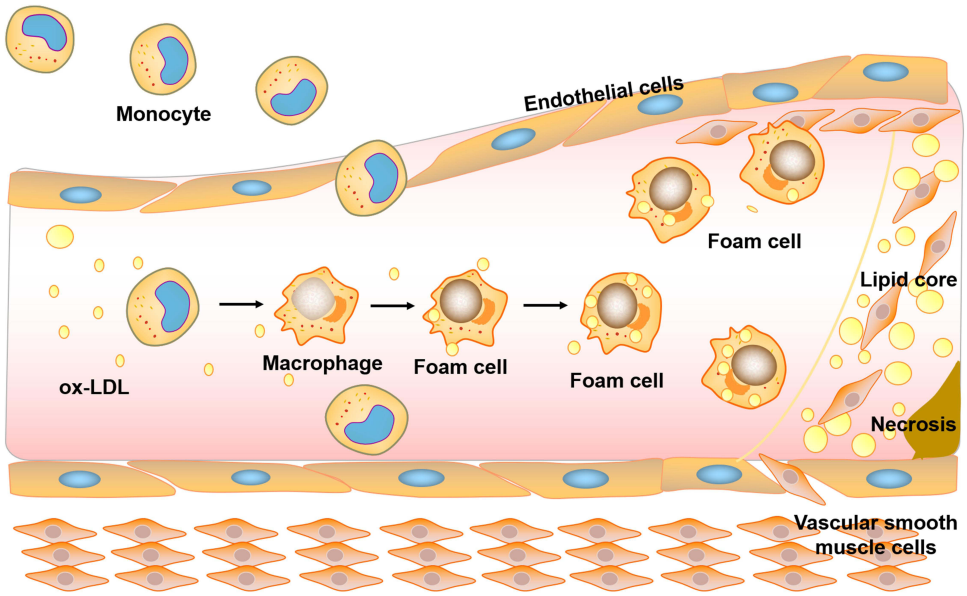

Figure 2 The development of atherosclerosis plaques.

scavenger receptor type A (SR-A), CD36, and lectin-like oxidized low-density lipoprotein receptor-1 (LOX-1). Foam cells and other immune cells secrete several cytokines (eg, IL-6, TNF-α, IL-1β, etc.). These cytokines can induce vascular smooth muscle cells (VSMCs) to migrate from tunica media into the tunica intima and proliferate. These differentiated VSMCs can phagocytize ox-LDL, form VSMC-derived foam cells and may produce extracellular traps which contributed to plaque progression by influencing the microenvironment of advanced plaques.[10–12] Other VSMCs secrete collagen or fibronectin to form fibrous cap. Subsequently, the macrophage-derived and VSMC-derived foam cells gradually form lipid core. Plaque rupture will eventually take place in lesions with large lipid core and thin fibrous cap, leading to platelet adherence, aggregation and thrombosis, causing severe clinical events.

The Underlying Mechanism-Reactive Oxygen Species (ROS)

The basic processes of ROS generation have been widely studied in recent years. It is commonly recognized that ROS generation is the predominant mechanism by which PDT exerted its effects. It is a plausible theory that ROS production is the major mechanism by which PDT-derived SDT functions. However, the difference between the two is that for PDT, the mechanisms of ROS generation due to photodynamic reaction are well identified, whereas for SDT, there are relevant hypotheses but none with certainty.

There are two photochemical interaction pathways to generate ROS—type I and type II.[13] In the type-I mechanism, the photosensitizer (PS) is excited by a specific wavelength of light before reacting with the substrate to produce free radicals and anionic radicals through a hydrogen atom or electron transfer procedure. Since most of the previously formed free radicals would react with oxygen, ROS in cells is generated through a chain of intricate free radical reactions. The main component of the type II mechanism is the interaction of PS excitation to the triplet state with oxygen molecules, and the formation of singlet oxygen. Both reactions could occur simultaneously, and the proportion of the procedures is determined by the type of PS employed, the substrate, and the concentration of oxygen.[14]

Although the mechanism underlying the generation of ROS is currently not well defined for SDT, there are two potential hypotheses that dominate the mainstream perspective—sonoluminescence (SL) and pyrolysis. Considering the application of sound-sensitizers that are simultaneously photosensitizers, such as protoporphyrin IX (PpIX) and 5-aminolevulinic acid (ALA),[15–18] SL is considered to be a key trigger for sonosensitizer-mediated ROS production in SDT. SL is a form of chemiluminescence, which is the phenomenon of light emission excited by the energy released by the rapid collapse of a bubble under ultrasonic excitation, and is based on the ability of ultrasound to generate cavitation.[19,20] Cavitation includes both inertial cavitation and stable cavitation.[21] SL occurs during the acoustic cavitation process, with inertial cavitation as the

dominant process. Following the collapse, SL, as well as chemicals in the surrounding medium, such as free hydroxyl radicals, are generated.[22] This is accompanied by destruction of cells and tissues to exert therapeutic effects. Therefore, it is essential to clarify the relationship between the cavitation dose and the generation of hydroxyl radicals. Peter et al assessed the creation of free radicals using the chemodose of hydrogen peroxide and showed that the higher the cavitation dose, the greater the generation of radicals.[23] Similar findings were reported by Villeneuve et al[24] In addition, Xu et al discovered that the reactive oxygen radicals were characterized by aqueous PpIX, and that the decomposition was inhibited by radical scavengers such as NAC, but not sodium azide, which showed that PpIX decomposition by ultrasound was determined by the hydroxyl radical.[25] It is well known that inertial cavitation dominated the SL; however, whether stable cavitation could cause SL deserves further investigation. Generally, stable cavitation indicates that the bubbles are underactive during chemical and SL processes. The presence of some bubbles is called "high-energy stable cavitation", and it has two properties—stable shape and an active state for SL or chemical reactions.[26] Furthermore, the mechanism of multi-bubble sonoluminescence (MBSL) has been widely accepted as a chemiluminescence phenomenon caused by excited OH radicals.[27] This has also been demonstrated in single-bubble acoustic chemistry studies. Yasui and his team demonstrated that O radicals were the main oxidants produced by gaseous bubbles; therefore, the generation of OH radicals subsequently triggered the same mechanism of ROS as PDT—Type I and II pathways.

A contrasting hypothesis is that the pyrolysis that occurs at the gas–liquid interfacial regions after sonoluminescence is the mechanism for the production of free radicals. There are three regions,[28,29] and using the ESR-spin trapping technique, the mechanisms underlying the assignment of free radical structures have been elucidated by numerous studies.[29,30] The first region is the gas phase that is generated by a collapsed cavitation bubble. When the intense bubble lapse occurs, the temperature within the bubble increases to 5000 Kelvin or even 15,000 Kelvin, accompanied by high pressures. This causes water vapor and oxygen to be dissociated into oxidants such as OH radicals and O radicals, which are generated inside the bubble.[20,30,31] For free radicals, a higher temperature inside the bubble is not always beneficial; there exists an optimal bubble temperature of approximately 5500 Kelvin for better production of free radicals. This is because the oxidants are consumed by nitrogen inside the bubble when the temperature is too high.[32] On the other hand, the temperature inside the bubble is dependent on a variety of factors, such as the thermal conductivity and heat capacity ratio in the bubbles, and a reduction in the heat capacity ratio would significantly decrease the temperature.[33] The gas–liquid interface area is the second region, which includes methyl radicals, phenyl, and tert-butyl radicals. The third region is the original solvent at room temperature, where the solute reacts with OH radicals and H atoms to produce radiation-chemistry-like byproducts.

Redox homeostasis is the system that maintains the balance between oxidation and antioxidation in the body.[34] Disruption of the balance is one of the pathological mechanisms of many diseases, such as AS, cancer, and cognitive impairment.[35–37] ROS plays an important role in oxidative stress, which is a collective term for a series of free radicals, including superoxide, hydroxyl, peroxide, and hydroperoxide.[38] ROS causes cellular damage, including oxidation of proteins, lipids, and carbohydrates, altering the genome and cellular structure, and acting as a signaling molecule to induce intracellular signaling pathway transduction.[39,40] In addition, the equilibrium between ROS generation and the capacity of cells to achieve antitonicity or rehabilitate damage could lead to oxidative stress and ultimately trigger different cell death mechanisms, including apoptosis, necrosis, and autophagy.[41,42] Multiple cell types, including endothelial cells, macrophages, foam cells, and VSMCs participate in the pathogenesis of AS,[43] and ROS contributes to its pathophysiological process by affecting these cell functions.[35] This is the mechanism that PDT and SDT exploit to develop great therapeutic potential for AS.

Photo-Based Energy-Conversion Nano-Therapy

Photothermal Therapy (PTT)

PTT can be beneficial for eradicating or reversing AS plaque, which is beyond the effect of modern therapies for AS, such as lipid-lowering drugs or recanalization operations. PTT involves two key elements—photothermal agents and laser radiation, which are typically near-infrared radiation (NIR). Different strategies have been applied to ensure that photothermal agents can be precisely guided and absorbed by the plaque deposits. The agents then convert light energy into heat, inducing intracellular hyperthermia. This process induces cell necrosis, apoptosis, and autophagy depending on the thermal energy or ROS produced in the process, thus preventing the rapid progression of AS. Various photothermal

agents have been used in AS, which can generally be categorized into two types—inorganic and hybrid nanoparticles (NPs). Inorganic NPs have small-sized effects and optical/magnetic/ultrasonic signal-response performance and may serve as better theranostic agents. Organic nanomaterials can be degraded and metabolized in vivo and have better biocompatibility, greater drug loading capability, and longer circulation time. Hybrid NPs usually combine the advantages of both organic and inorganic materials; thus, they have attracted great interest in recent years.[44]

Inorganic Photothermal Agents

Initially, Lukianova-Hleb et al proved that gold NPs generated photothermal microbubbles around the lesion in vitro with a short laser pulse and were able to disrupt plaque tissue mechanically, without damaging the arterial wall.[45] Gold NPs can be phagocytosed by macrophages at sites of vascular inflammation, and their vitality will not be affected unless exposed to NIR laser.[46] In apolipoprotein E knockout (ApoE-/-) mice (an animal model used to mimic AS), gold nanorods (Au NRs) were applicable as both contrast agents for computed tomography (CT) imaging and photothermal agents for inflammatory macrophages irradiated by an 808 nm laser.[47] However, noble metal nanostructures are expensive and experience obvious deformation under continuous irradiation, which eventually impairs their photothermal ability. Materials such as graphene and carbon nanotubes are much more reliable. Single-walled carbon nanotubes (SWNTs) are engulfed by 94 ± 6% of macrophages and induced 93 ± 3% in vitro cell death under irradiation; however, the nonspecific uptake of SWNTs would damage other organs, thus requiring more researches to improve their accuracy.[48]

Semiconductor photothermal nanomaterials have a number of advantages, including lower cost, simpler synthetic procedures, and better photothermal effect. Ultrasmall $CuCo_2S_4$ nanocrystals exhibit high photothermal conversion rate and can be rapidly cleared by the renal system.[49] In addition, MoO_2 nanoclusters can also eliminate macrophages with no serious side-effects in vivo under NIR.[50] The photothermal conversion efficiency of Cu_3BiS_3 nanocrystals is up to 58.6% with a power density of 0.4 $W \cdot cm^{-2}$, and they can also be applied as a CT contrast agent to evaluate carotid inflammation.[51] Janus heterodimers consisting of noble metal and semiconductor, such as the Janus Ag/Ag_2S beads synthesized by Peng et al, possess better photothermal conversion efficiency, lower cytotoxicity and better biocompatibility than the individual components. They can be uptake by macrophages and remarkably eliminate these cells from arterial inflammation without further damage to the normal arterial wall and major organs.[52]

Hybrid NPs

With the development of nanotheranostics, the construction of multifunctional NPs has become increasingly feasible. To make photothermal agents target different cells more precisely, they are coated with receptor-specific antibodies or signal molecules. Drugs that play a protective role in AS have also been loaded to strengthen their therapeutic effects on restoring the endothelial function. Some materials are combined with nanomotors that can help NPs penetrate deeper into the lesion. Last but not least, combination of nanomaterials that can strengthen imaging resolution enables image-guided PTT.

SR-A is expressed by activated macrophages in AS plaque, which can be competitively blocked by dextran sulfate (DS) and inhibit the cellular endocytosis of ox-LDL. A multifunctional therapeutic nanoplatform, CS-CNCs@Ce6/DS, possesses rapid photothermal conversion ability of chitosan-coated carbon nanocages (CS-CNCs) and enables efficient PTT. The nanoplatform further induces the PDT effect on the activated macrophages, as it gradually releases chlorin e6 (Ce6) in the lesion, reducing secretion of pro-inflammatory cytokine and alleviating proliferation and migration of VSMCs.[53] Oh et al synthesized mannosylated-reduced graphene oxide (Man-rGO) to enhance the therapeutic effect of graphene oxide, as it could bind to the mannose receptor, a marker of M2 macrophages that mediated phagocytosis.[54] To realize synergistic treatment effect of drugs and PTT, Liu et al used dendritic mesoporous silica NPs as nanocarrier to cap anticoagulant drug heparin (Hep) and copper sulfide (CuS), which provided a photothermal effect. Meanwhile, the hyaluronic acid (HA) bounding to the nanocarrier enabled it to release drugs according to pH and specifically target CD44-positive macrophages.[55] Transient receptor potential vanilloid subfamily 1 (TRPV1) is a thermo-sensitive channel in VSMCs, which induces a Ca^{2+} influx when the local temperature increases, further activating autophagy (Figure 3A (a)). Gao et al used copper sulfide (CuS) NPs coupled with antibodies of TRPV1 (Figure 3A(b)) as a photothermal switch to activate TRPV1 signaling (Figure 3A(c)), induced autophagosome formation (Figure 3A(d)), reduced lipid uptake, and

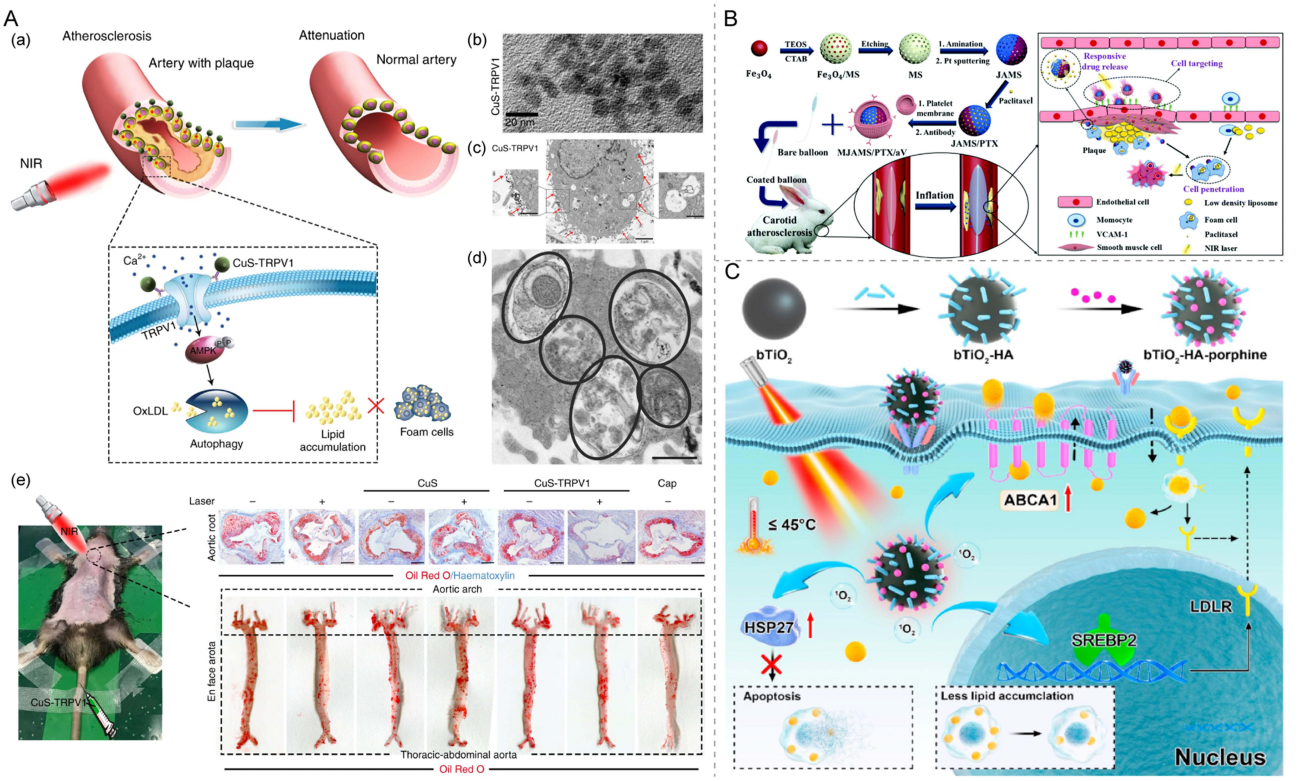

Figure 3 (**A**) (a) Illustration of CuS-TRPV1 switch for photothermal activation of TRPV1 signaling to attenuate atherosclerosis. (b) Transmission electron microscopy (TEM) image of CuS-TRPV1. (c) Representative TEM images of targeting of CuS-TRPV1 to VSMCs membrane rather than endosome or lysosome. Red arrows: localization of nanoparticles. (d) Representative TEM image of autophagosomes in VSMCs after photothermal activation of TRPV1 by CuS-TRPV1. Black circles: double-membrane structures of autophagosomes. (e) NIR laser treatment and representative images of Oil Red O-stained aortic root sections and complete aorta. Reproduced from Gao W, Sun Y, Cai M, et al. Copper sulfide nanoparticles as a photothermal switch for TRPV1 signaling to attenuate atherosclerosis. *Nat Commun*. 2018;9(1):231, with permission under the terms of the CC-BY license.[56] Copyright 2018, Springer Nature. (**B**) Schematic illustration of the synthesis process of MJAMS/PTX/aV and the mechanism of treatment of atherosclerosis using the MJAMS/PTX/ aV coated balloon. Reproduced with permission from Huang Y, Li T, Gao W, et al. Platelet-derived nanomotor coated balloon for atherosclerosis combination therapy. *J Mater Chem B*. 2020;8(26):5765–5775. Copyright 2020, Royal Society of Chemistry.[57] (**C**) Schematic illustration of lipid metabolism in foam cells after phototherapy with bTiO2-based nanoprobes irradiated by 808 nm NIR laser. Reprinted from *Bioact Mater*, 17, Dai T, He W, Tu S, et al. Black TiO(2) nanoprobe-mediated mild phototherapy reduces intracellular lipid levels in atherosclerotic foam cells via cholesterol regulation pathways instead of apoptosis. 18–28. With permission under the terms of the CC-BY license.[58]

thus prevented VSMCs from turning into foam cells. In vivo experiment exhibited significant reduction of lesion areas, indicating great therapeutic effect of AS (Figure 3A(e)). [56]

Using different imaging contrast, NIR radiation under guidance benefits precise treatment toward criminal lesions. Chen et al developed a polymeric nanosystem (V-PPZ-NPs) that encapsulated phthalocyanine zinc (ZnPc) and perfluorohexane (PFH) and conjugated it to an anti-VEGFR-2 antibody so that it could target the vascular endothelial growth factor receptor (VEGFR-2) on vascular endothelial cells (VECs), since inhibition of neovascularization could help stabilize atherosclerotic plaque and prevent cardiovascular events. The NPs can be observed in vivo by ultrasound and photoacoustic (PA) imaging. Thus, laser irradiation can be guided to the optimal location to kill the surrounding cells.[59] Another nanosystem targeting VECs in the same way utilizes 3 nm $MnFe_2O_4$, PFH and polylactic acid-glycolic acid (PLGA) shells to realize magnetic resonance imaging (MRI) T1 and T2 imaging except for PA imaging and ultrasound molecular imaging.[60]

Several studies have shown that photothermal agents made of nanomotors can deeply penetrate target lesions owing to their self-propelled motion ability and combination with biomolecules such as anti-vascular cell adhesion molecule-1 (anti-VCAM-1) antibodies (aV), which target overexpressed VCAM-1 in AS plaque. Huang et al constructed a nanomotor of mesoporous silica (MS) and platinum (Pt), which was loaded with the anti-proliferative drug paclitaxel (PTX), and coated with a platelet membrane to prevent drug leakage (Figure 3B). Under NIR irradiation, Pt provided immediate elimination of inflammatory macrophages and drove the nanomotor to penetrate the lesion for drug retention, achieving long-term anti-proliferation effects.[57] A similar micromotor MMS/Au/PTX/VEGF/aV designed by Li et al promoted extra short-term

endothelialization by releasing vascular endothelial growth factor (VEGF).[61] Another type of nanomotor was mainly composed of L-arginine (LA), β-cyclodextrin (β-CD) and Au which had dual-power source. LA induced the generation of NO which could not only work as a driving force but also restore endothelial function and decrease oxidative stress, while Au could provide additional thermophoresis power under irradiation. In vivo, the dual-mode nanomotor showed better enrichment in plaque area than the single-mode one and led to fewer lesions after two months of treatment.[62]

Considering the irreversible damage to tissues caused by high thermal exposure and the risk of plaque destabilization raised by cell apoptosis itself, Dai et al designed a nanoprobe (bTiO2-HA-p) that allowed simultaneous PTT and PDT with a single NIR laser excitation, which resulted in a relatively low temperature (44.5 °C). This temperature could prevent cell apoptosis through activation of HSP27, promote ABCA1-dependent cholesterol efflux, and reduce SREBP2-induced biosynthesis of LDLR, thus decreasing uptake of lipid (Figure 3C). The nanoprobes attenuated as much as 12.8% of intracellular lipid accumulation compared to 5% and 3% of single PTT and PDT functional nanoprobes, respectively.[58]

Most photothermal agents are stimulated under laser irradiation with the first near-infrared window (NIR-I 700−950 nm), while the NIR-II (1000–1700 nm) laser has better tissue penetration ability and higher maximum permissible exposure than NIR-I. Copper sulfide (CuS) can be excited in the NIR-II region and deeply penetrate the lesions, thus Cao et al developed HA- and PEG-modified CuS/TiO_2 heterostructure nanosheets (HA-HNSs), which combined SDT and PTT for early atherosclerotic treatment and inhibited atherosclerotic plaque progression, with no obvious toxicity.[63]

A Clinical Trial of PTT

So far, there has only been one clinical trial of PTT on AS. Based on the promising outcomes of a preclinical trial on 101 Yucatan miniature swine,[64] Kharlamov et al conducted the NANOM-FIM trial to evaluate the safety and feasibility of PTT mediated by NPs in patients with coronary artery disease with flow-limiting plaque. In the two experimental groups, silica-gold NPs were delivered in a bioengineered on-artery patch and the silica-gold iron-bearing NPs were transferred with targeted microbubbles and stem cells using a magnetic navigation system, while patients in the control group were treated with standard stent implantation.

The ongoing clinical follow-up analyzed the event-free survival and exhibited a significantly lower risk of cardiovascular death in the first group than in the others (91.7% vs 81.7% and 80%, respectively; $p < 0.05$), and no complications associated with the target lesion occurred.[65] A subsequent 5-year observational prospective cohort analysis of the NANOM-FIM trial illustrated that PTT with silica-gold NPs was safe with lower mortality, fewer major adverse cardiovascular events, and better revascularization of the target plaque compared to that with stent implantation. Efficient regression of coronary AS suggested a high potential to introduce PTT with silica-gold NPs in clinical practice. However, the trial also raised questions like nanotoxicity of the iron-bearing NPs and undesirable distribution in other tissue and organs, which were the major limitations for the development and implementation of nanotechnique in real clinical practice.[66]

Photodynamic Therapy (PDT)

Although the feasibility of PTT in macrophage elimination has been proven, a variety of obstacles, such as accuracy, stability, and pharmacokinetics, still need to be overcome before clinical practice. PDT is a promising alternative to PTT and is composed of photosensitizers which can accumulate selectively in lesions and laser irradiation to induce local therapy. Under irradiation at the maximum absorption wavelength of the photosensitizer, energy is transformed and leads to ROS generation within the lesion, which induces cell death through different pathways. Thus, PDT can help stabilize and reduce plaque size, enlarge the stenosis vessel, and prevent occlusion, further prevent serious situations such as acute coronary syndrome.[67]

To date, there have been three generations of photosensitizers. The first generation includes hematoporphyrin derivative (HpD) and photofrin II (a purified form of HpD). The majority of second-generation compounds are derived from porphyrin structures, such as benzoporphyrins, phthalocyanines, and PpIX, whereas others, including mono-aspartyl chlorin e6 (NPe6), temoporfin, and pheophorbide derivatives, are related to the chlorin structure. These agents possess a clear composition and better light-absorption capability. The third generation uses nanotechnology to combine traditional photosensitizers with nanomaterials and different drugs for AS, so that they have higher efficacy of energy transformation, better accuracy, and various functions.[68]

The First Generation

In 1983, Spears et al suggested that hematoporphyrin derivative (HpD) could not only be used clinically to localize malignant neoplasms but also be concentrated selectively within atherosclerotic plaque in both rabbits and Patas monkeys.[69] Since its introduction into this field, HpD has been shown to induce quantitative changes in atheroma in thoracic aortic segments under 636 nm light irradiation.[70] Intravascular irradiations in vivo after HpD injection can inhibit the growth of smooth muscle cells (SMCs) and the intimal hyperplasia response, improving restenosis after angioplasty.[71] In addition, the rapid increase in HpD concentration upon local application makes it possible to use PDT to prevent restenosis after angioplasty without serious side-effects.[72]

Neave et al proved that in comparison to the normal arterial wall, AS plaque took up more dihematoporphyrin ether (photofrin II), especially 48 hours after the injection, and the plaque showed significant reduction 6 weeks after PDT.[73] It is proved that morbid SMCs are more sensitive to PDT than healthy cells both in vitro and in vivo, confirming the feasibility of photofrin II–induced PDT.[74,75] Several experiments have been conducted to determine the most appropriate dose and light intensity that can avoid extensive vascular injury and fully ablate plaque.[76–78] Amemiya et al found that photofrin-mediated PDT using the pulse wave yttrium aluminum garnet-optical parametric oscillator (YAG-OPO) laser had better outcomes than a continuous-wave argon dye (Ar-dye) laser, penetrating deeper into the media of the vessel wall.[79] However, the complex composition of the first generation was not good for the specificity and stability of the damage intensity, which limited the clinical exploitation and necessitated the development of the second generation.

The Second Generation

Verteporfin, a benzoporphyrin derivative monoacid ring A (BPD-MA), may have a better treatment effect than HpD, because its maximal absorption is at 692 nm, which is beyond the absorption spectrum of blood at 630 nm. BPD-MA can be preferentially taken up by atherosclerotic plaque both in vitro and in vivo,[80] and this process can be enhanced when it is combined with plasma lipoproteins.[81] Jain et al performed intra-arterial administration of liposomal verteporfin and intra-arterial light irradiation in ApoE-/- mice, inducing dramatic macrophage apoptosis in the plaque.[82] Another porphyrin-like chemical, hematoporphyrin monomethyl ether (HMME), induces apoptosis of macrophages through the caspase-9 and caspase-3 activation pathways, and may become feasible for unstable AS plaque.[83]

5-Amino-levulinic acid-induced protoporphyrin IX (ALA-PpIX) is a naturally occurring porphyrin precursor, which produces PpIX to sensitize the target cells under irradiation. Based on various animal models[84–87] and clinical studies,[88] its efficacy in depleting the VSMC population and inhibiting intimal hyperplasia or constrictive remodeling has been demonstrated. However, ALA can cause hemodynamic changes (reductions in systemic and pulmonary pressure and lung resistance), which may limit its use in the cardiovascular field.[89]

Eldar et al first demonstrated that porphyrin-based copper phthalocyanine tetrasulfonate, a water-soluble phthalocyanine dye, preferentially accumulated in atheromatous plaque in rabbits.[90] In vitro, when fluoride is added before exposure to light, chloroaluminium phthalocyanine (AIPc) and its derivatives can selectively destroy SMCs without affecting endothelial cells and skin fibroblasts, without causing cutaneous phototoxicity, which is the most common side-effect of photosensitizers.[91] Later, de Vries et al found that ox-LDL could deliver AlPc specifically to macrophages in the plaque, mediated by scavenger receptors.[92] Indocyanine green (ICG) has also been promising for the treatment of restenosis of carotid arteries under extracorporeal light irradiation because of the better tissue penetration of NIR light.[93]

The photosensitizer, mono-L-aspartyl chlorin e6 (NPe6), specifically deposits in the AS plaque[94] and can be eradicated soon after intravenous injection, so it is less likely to photosensitize the skin, which is a common side effect for photosensitizers. Hayashi et al proved that NPe6 excited by irradiation could destroy the construction of the elastic fiber network and dissociate ester bonds of cholesterol esters in the plaque.[95] Chlorin (Ce6) covalently attaches to bovine serum albumin can be recognized and internalized by class A Type-I scavenger receptors on macrophages.[96] Ce6 can be released by cathepsin-B-activatable theranostic agent (L-SR15) and can not only provide diagnostic visualization but also eliminate macrophages selectively under laser irradiation, attenuating cathepsin B activity to stabilize the plaque.[97] However, cardiovascular drugs such as atorvastatin and clopidogrel, which are often prescribed for patients with AS, have undesirable effects on photosensitizers, significantly affecting photosensitization in vitro without interfering with the cellular uptake of L-SR15.[98] Weiss-Sadan et al also designed a photosensitizing quenched activity-based probe to

target cysteine protease cathepsin that was typically expressed in arterial lesions and decreased the number of macrophages without affecting SMC and collagen contents.[99]

Another chlorin-based second-generation photosensitizer, motexafin lutetium, is also effective for AS. Irradiated by 732 nm light (2 J/cm^2), motexafin lutetium produces cytotoxic singlet oxygen and leads to changes in mitochondrial membrane potential (MMP), release of cytochrome c, and activation of the caspase family. This process leads to phosphatidylserine externalization and induces apoptotic DNA fragmentation.[100] Motexafin lutetium has been proved to target and significantly reduce atherosclerotic lesions of both vein graft intimal hyperplasia and graft coronary artery disease.[101,102]

With pheophorbide derivative PH-1126, which is selectively deposited in AS plaque, foam cells can be expelled from the endothelium to the intimal surface of the plaque.[103] Pyropheophorbide-alpha methyl ester (MPPa)-mediated PDT generates ROS and induces apoptosis of RAW264.7 cells, while the damage level is related to the dose of light irradiation.[104] Synthesized CTSB-PPP that can be cleaved by cathepsin B in plaque, releases pheophorbide a, and selectively destroys cells with high cathepsin activity upon irradiation.[105] Wang et al discovered that curcumin (CUR)-mediated PDT could mediate autophagy in VSMCs treated with ox-LDL, further inhibiting the phenotypic transformation, migration, and formation of foam cells in vitro.[106]

The Third Generation

Dendrimers exhibit relatively low cytotoxicity and good biocompatibility with nanomaterials as drug carriers. Polyamidoamine (PAMAM) dendrite delivery of a ZnPc photosensitizer is found to be considerably aggregated on AS plaque against healthy tissue.[107] ALA dendrimers enhance porphyrin synthesis and have higher affinity with macrophages than endothelial cells, which is mainly mediated by caveolae-mediated endocytosis.[108] Cespedes et al later proved that ALA dendrimers exhibited selective PDT response on foam cells rather than endothelial cells as well.[109] Wennink et al encapsulated temoporfin in polymeric micelles to realize the selective elimination of macrophages and alleviate side-effects, though the instability of the system might be great obstacles for clinical use.[110]

Chlorin-based photosensitizers are one of the most popular study objects in third-generation photosensitizers because they can result in fluorescence emission and provide NIR fluorescence imaging with a high target-to-background ratio. Ce6 is conjugated to HA to form macrophage-targeted theranostic nanoparticles (MacTNP), which releases Ce6 and becomes phototoxic upon illumination inside activated macrophages in vitro, as excess ROS degrades the NPs.[111] As shown in Figure 4A(a), Song et al combined dextran sulfate (DS) to Ce6, which could be engulfed by activated macrophages and foam cells via SR-A-mediated endocytosis. Optical imaging-guided DS-Ce6 photoactivation can detect inflammatory activity in plaques in vivo and simultaneously reduce plaque burden and inflammation by inducing apoptosis, autophagy (Figure 4A(b)), and efferocytosis.[112] With the triple-helix structure of beta-glucan (Glu), Glu/Ce6 nanocomplexes can be recognized by the dectin-1 receptor of macrophages to mediate efficient membrane destruction and apoptosis of foam cells under irradiation.[113]

Upconversion nanoparticles (UCNPs) are helpful for the shallow penetration depth of Ce6 owing to their ability to convert NIR light into visible light and can be used for noninvasive imaging of deep tissues, drug delivery, and PDT. UCNPs-Ce6 can induce translocation of the proapoptotic factor Bax, release of cytochrome C, and upregulation of other apoptotic factors such as cleaved caspase-3/9 under laser irradiation, which leads to the apoptosis of THP-1 cells.[116] ROS generated during UCNPs-Ce6-mediated PDT also activates the PI3K/Akt/mTOR signaling pathway which enhances autophagy, promotes cholesterol efflux through ABCA1 (Figure 4B), [114] and inhibits the expression of pro-inflammatory factors in M1 peritoneal macrophages,[117] suggesting that it may help relieve the lipid burden of plaque in vivo. Ma et al designed a platelet membrane-coated nanostructure (PAAO-UCNPs) containing UCNPs and Ce6 for accurate localization of plaque and noninvasive PDT of AS. Platelet membrane coating facilitates the specific targeting of the therapeutic system to macrophage-derived foam cells.[118]

Xu et al constructed theranostic nanoprobes, TPZ/IR780@HSA-OPN, in which HAS-OPN referred to human serum albumin (HAS) decorated with a high-affinity peptide targeting osteopontin (OPN), an overexpressed marker of foam cells in atherosclerotic plaque. The nanoprobes encapsulated the photosensitizer IR780 and hypoxia-activatable tirapazamine (TPZ), implementing biological suppression of foam cells under less oxygen content induced by PDT. Under the

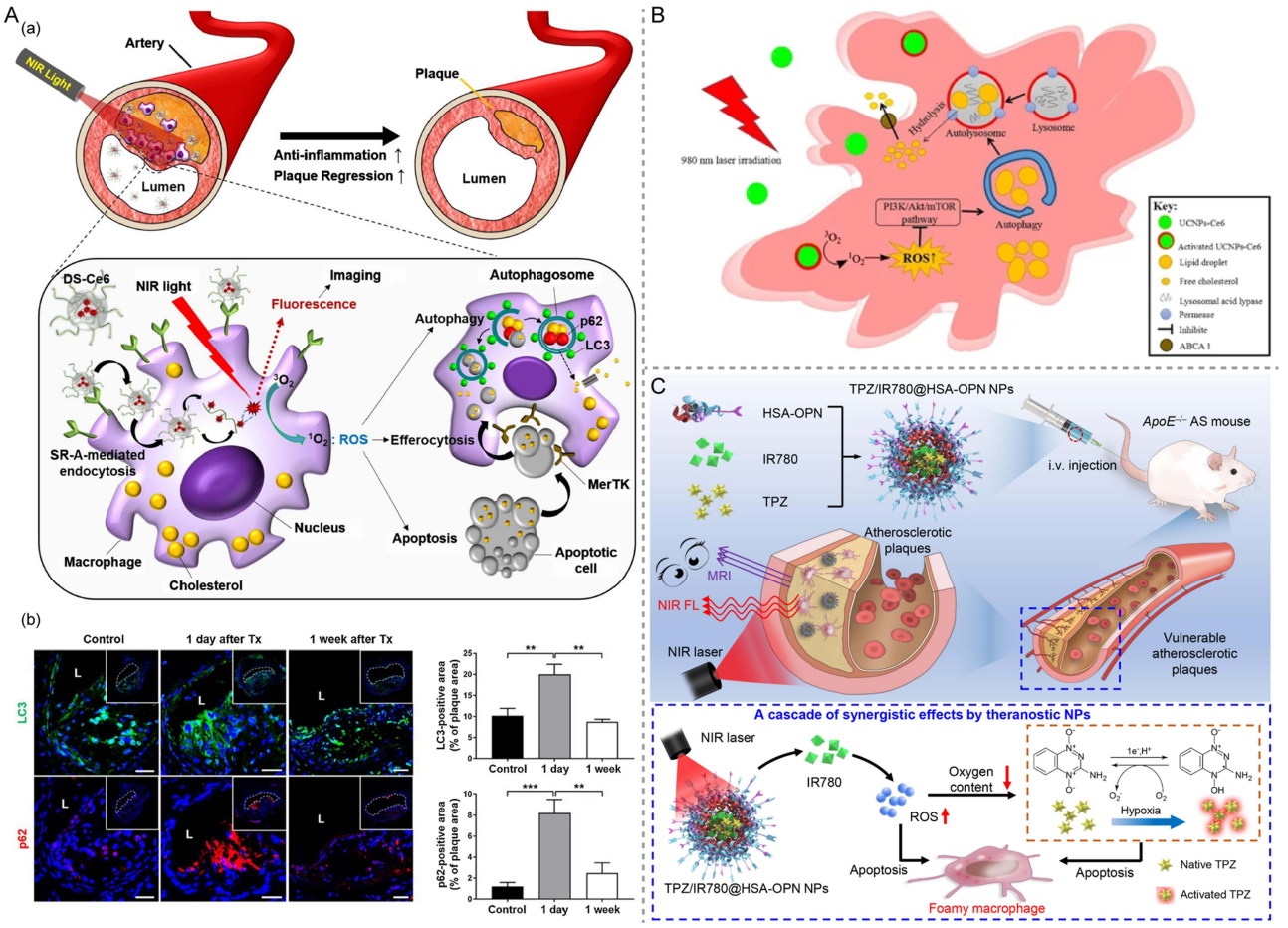

Figure 4 (**A**) (a) Schematic overview of photoactivation activated by DS-Ce6 targeting macrophage SR-A for autophagy induction and efferocytosis enhancement to regress atherosclerosis. (b) Confocal laser scanning microscopy images of the double IF of autophagy marker LC3 (green) and p62 (red) at 1 day and 1 week after treatment. Blue: nucleus stained with DAPI. **: $P < 0.01$, ***: $P < 0.001$. Reproduced with permission from Song JW, Ahn JW, Lee MW, et al. Targeted theranostic photoactivation on atherosclerosis. *J Nanobiotechnology*. 2021;19(1):338. under the terms of CC-BY license. Copyright 2021, Springer Nature.[112] (**B**) Schematic diagram of UCNPs-Ce6-mediated PDT and the mechanism of autophagy. Reproduced with permission from Han XB, Li HX, Jiang YQ, et al. Upconversion nanoparticle-mediated photodynamic therapy induces autophagy and cholesterol efflux of macrophage-derived foam cells via ROS generation. Cell Death Dis. 2017;8(6):e2864. under the terms of CC-BY license. Copyright 2017, Springer Nature.[114] (**C**) Schematically illustrate construction of theranostic TPZ/IR780@HSAeOPN NPs, which could precisely regress the vulnerable atherosclerotic plaques through a cascade of synergistic events triggered by careful lasers irradiation under the guidance of NIR fluorescence/MR imaging. Red "up" arrow refers to the decreased content of oxygen, and the red "down" arrow indicates the increase of ROS. Reprinted from Acta Pharm Sin B, 12(4), Xu M, Mao C, Chen H, et al. Osteopontin targeted theranostic nanoprobes for laser-induced synergistic regression of vulnerable atherosclerotic plaques. 2014–2028. Copyright 2022, with permission from Elsevier B.V.[115]

guidance of fluorescence/MR imaging, the nanoprobes can greatly regress the vulnerable plaque and decrease the degree of carotid artery stenosis in vivo[115] (Figure 4C).

Despite the extensive clinical use of interventional laser irradiation, the application of PDT without external light irradiation presents an exciting field. Mu et al designed a chemiexcited system (FeCNPs) that also possessed T1-weighted contrast ability. In vivo MRI and in vitro experiments have shown that FeCNPs can accumulate in plaque and effectively eliminate macrophages, reducing plaque size and thickness.[119]

Clinical Research

Adjuvant photofrin-mediated PDT was performed in five patients undergoing coronary stent deployment. Photofrin was administered using a local delivery balloon catheter to the stent-implanted lesions. After follow-up for eighteen months, no major adverse effects (myocardial infarction, coronary artery spasm, thrombosis, dissection, or aneurysmal dilatation) or in-stent restenosis were detected.[120] In 1999, Jenkins et al investigated the effect of adjuvant ALA-mediated PDT after femoral percutaneous transluminal angioplasty (PTA). Seven patients with symptomatic restenosis or occlusion at the same site after the first conventional angioplasty were enrolled in the study. After oral administration of 5-ALA, adjuvant

PDT was performed using a laser fiber within the angioplasty balloon, following a second femoral PTA. No adverse complications, death, or no restenosis occurred, suggesting the safety and the potential for restenosis prevention of endovascular PDT following PTA.[88] Rockson et al demonstrated the safety and underlying therapeutic effects of motexafin lutetium in 47 patients with peripheral arterial AS. At follow-up, there were no deleterious vascular effects, and the standardized classification of clinical outcomes showed improvement in 29 patients (62%), no change in 17 patients (36%), and moderate worsening in 1 patient (2%).[121] Another study was conducted in 75 patients undergoing percutaneous coronary intervention (PCI) and stent implantation, by following them for 6 months and confirmed that motexafin lutetium-mediated PDT was safe as an adjunct to PCI and established a well-tolerated maximum dosage and range of light doses.[122] All the clinical trials mentioned have been conducted in a small sample size which leads to a less convincing result; thus, we need more large cohort studies to provide precise and comprehensive information of treatment effect and side effect.

Ultrasound-Based Energy-Conversion Nano-Therapy

The application of PDT and PTT raises the question of their effectiveness being limited by their relatively shallow penetration depth of light through tissue, and concentration on superficial lesions.[123] Sonodynamic therapy (SDT), which originates as a proxy for PDT, is a perfect solution to the problem as ultrasound provides deep tissue penetration. SDT uses low-frequency and low-intensity ultrasound to activate sonosensitizers, which yields localized cytotoxicity mainly through the generation of ROS. It is interesting that many photosensitizers can also be applied as sonosensitizers. SDT was first used in 1989, proposed by Umemura et al[124] and has been widely investigated for the treatment of tumors. Because light can be absorbed in the blood to some extent, SDT has become a prospective alternative to PDT for stabilizing and reducing the size of atherosclerotic plaque. In 2002, Arakawa et al reported that SDT could prevent neointimal hyperplasia after iliac artery stent implantation in rabbits, suggesting that SDT might have great clinical value in the treatment of cardiovascular disease.[125] Sonosensitizers that have been investigated for AS include porphyrin derivatives, herbal-derived agents, and agents combined with nano materials.

Porphyrin Derivatives

Many photosensitizers, especially porphyrin derivatives, can also be applied as sonosensitizers. PpIX-mediated SDT can produce intracellular singlet oxygen and lead to cytoskeleton disruption and apoptosis of THP-1 macrophages in vitro,[15] as well as significantly induce membrane permeabilization and facilitate the entry of drug into macrophages. This process promotes the anti-atherosclerotic effect of atorvastatin on THP-1-derived foam cells, including reduction of intracellular lipid droplets and increasing in cholesterol efflux by upregulation of PPARγ and ABCG1 expression.[126]

A large number of cytological experiments have already proved that 5-ALA-mediated SDT (ALA-SDT) can alleviate the burden of AS plaque, mainly by inducing apoptosis and autophagy of macrophages. For example, ALA-SDT induces ROS generation and a significant loss of MMP in vitro.[127] Chen et al found that, in ALA-SDT, voltage-dependent anion channel 1 (VDAC1) led to Ca^{2+}-mediated oxidative stress[128] and mitochondria-caspase pathway and further accelerated the apoptosis of macrophages.[129] Under the irritation of ALA-SDT, other potential mechanisms include the caspase-3/8 pathway[17] and mitochondrial 18 kDa translocator protein (TSPO)[130] that induces apoptosis, PPARγ-LXRα-ABCA1/ABCG1 pathway that promotes efferocytosis,[131] ROS-AMPK-mTORC1 pathway that promotes autophagy[132] and the increased heme oxygenase-1 (HO-1) expression that reduces ox-LDL-mediated impairment.[133] Apart from macrophages, ALA-SDT also influences the equilibrium between different T lymphocyte subtypes and facilitates a switch toward Th2 polarization, which helps stabilize the plaque.[18] In vivo ALA-SDT experiment performed both in rabbits and ApoE-/- mice suggested that the treatment eliminated macrophage and inhibited matrix degradation, which helped inhibit plaque progression and decrease the occurrence of plaque disruption.[133,134] Increased mean lumen area and reduced artery stenosis also suggested that ALA-SDT was superior to treatment with atorvastatin alone, the standard of care for AS.[135]

Sinoporphyrin sodium (DVDMS) is also a porphyrin derivative which has been validated in SDT for AS. In plaque with high inclination to intraplaque hemorrhage, DVDMS-SDT can reduce iron retention by increasing ferroportin 1 (Fpn1) expression and activate the ROS-Nrf2-FPN1 pathway to reduce levels of the unstable iron pool and ferritin expression.[136] Meanwhile, the process inactivates the expression of CD47 to promote efferocytosis, thereby reducing inflammation.[137] In

both rabbits and mice experiments, arterial inflammation and angiogenesis were conspicuously alleviated after DVDMS-mediated SDT, which was similar to the treatment outcome of intensive statin treatment for 3 months.[138]

Herbal Derived Agents

Emodin, an anti-inflammatory agent, is found to be an effective sonosensitizer that induces the dissociation of intracellular filaments, aggregation of cytoskeleton proteins, and subsequent destruction of the cytoskeleton after SDT.[139]

Curcumin, extracted from the traditional Chinese herb Curcuma longa, has been shown to have the same effect on THP-1 cells under pulsed ultrasound irradiation (2 W/cm^2 with 0.86 MHz).[140] Hydroxyl-acetylated curcumin (HAC) removes the unstable hydroxy groups of curcumin[141] and induces autophagy in THP-1 macrophages through the ROS-dependent PI3K/AKT/mTOR pathway with decreased lipid accumulation.[142] Hydroxysafflor yellow A-mediated SDT causes autophagy in the same way.[143] Berberine-mediated SDT works in the same way and increases cholesterol efflux in either macrophages or foam cells.[144]

Li et al found that hypericin (HY)-mediated SDT produced ROS, promoted translocation of BAX from the cytosol to the mitochondria, and released cytochrome C, thereby inducing macrophage apoptosis.[145] Pseudohypericin (P-HY)-SDT has a similar function[146] and triggers the translocation of transcription factor EB (TFEB) from lysosome to nucleus, which promotes autophagy and lysosome regeneration. This process inhibits lipid uptake by reducing CD36 and SR-A expression, and enhances ABCA1 expression, which increases the release of free fatty acids, further decreasing the lipid burden of macrophages.[147]

Agents Combined with Nano Materials

Gonçalvez et al synthesized ALA:AuNPs, which could be used as both photosensitizers and sonosensitizers. AuNPs could help increase ROS generation and improve ROS function. SDT with ALA:AuNPs showed better results than PDT alone, as it decreased the viability of macrophages by 87% in 2 min.[148] SDT using the methyl ester of aminolevulinic acid (MALA) with AuNPs showed similar results in the reduction of macrophages.[149]

Curcumin nanosuspensions using polyvinylpyrrolidone (PVPK30) and sodium dodecyl sulfate (SDS) as stabilizers possess better water solubility and bioavailability than curcumin and can decrease total cholesterol (TC) and LDL, leading to transdifferentiation from M1 to M2 macrophages.[150]

Yao et al fabricated PFP-HMME@PLGA/$MnFe_2O_4$-ramucirumab nanoparticles (PHPMR NPs), which could also serve as a contrast agent for MRI/photoacoustic/ultrasound imaging and were able to inhibit neovascularization (Figure 5A). Under low-intensity focused ultrasound irradiation and multimodal imaging guidance, PHPMR NPs mediated SDT targeted to the mitochondria of VECs in the plaque, promoted apoptosis by ROS-induced caspase activation, and suppressed proliferation and migration, further reduced neovascularization and stabilized vulnerable plaques (Figure 5B). [151]

Clinical Research

Among the sonosensitizers mentioned above, the comprehensive mechanism and efficacy of ALA have made it the best choice for clinical trials. ALA-SDT has been performed mainly for peripheral AS diseases with great therapeutic results. A pilot clinical trial recruited 16 participants with peripheral AS and divided them into two groups. Atorvastatin was administered alone in one group, and a combination of atorvastatin and ALA-SDT was implemented in another. The combination therapy successfully decreased the ratio of vessel diameter to stenosis at 4 weeks, and the decrease was maintained until 40 weeks, indicating efficient regression of atherosclerotic lesions.[135] Nonetheless, strict RCT with larger sample size has to be conducted to eliminate the side effects of ALA on hemodynamics, while prolonged follow-up is necessary to state better long-term outcomes of SDT than modern treatment.

DVDMS-SDT had also been in a pilot clinical study, in which the researchers used contrast-enhanced ultrasonography analysis and fludeoxyglucose F18-positron emission tomography-computed tomography (PET-CT) to evaluate the reduced neovascularization and arterial inflammation, respectively. The beneficial effect after 1-month treatment was almost equivalent to the therapeutic outcome after 3-month intensive statin treatment, with no side effects in follow-up screening, indicating DVDMS-SDT alone or in combination with a reduced statin dosage might have lesion-specific

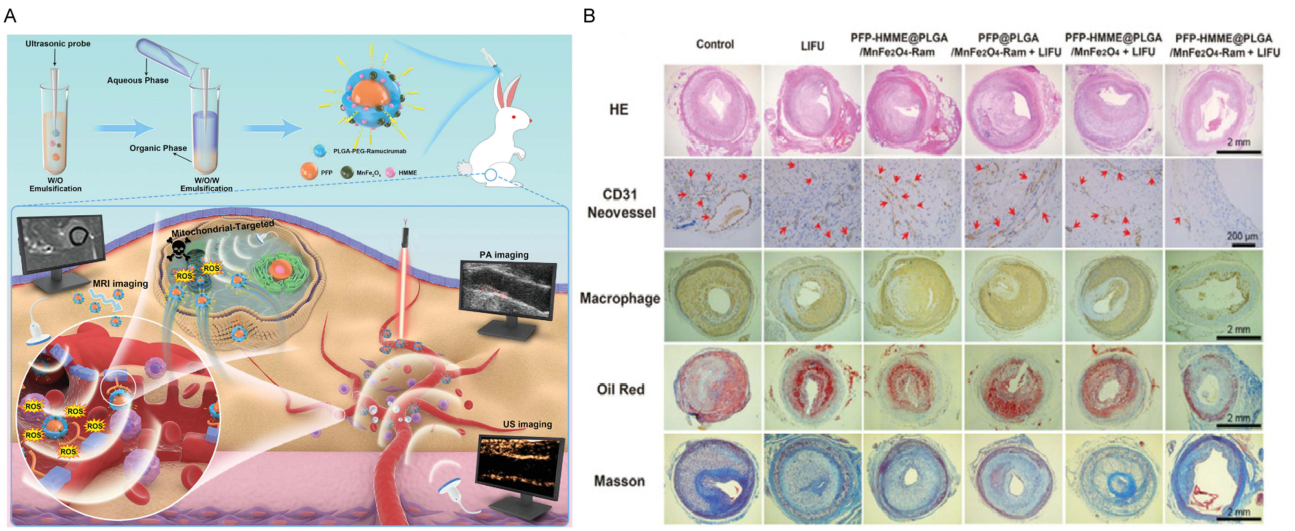

Figure 5 (**A**) Schematic illustration of the synthetic process for PFP–HMME@PLGA/MnFe2O4–Ram nanoplatform and the corresponding theranostic functionality for targeted MRI/PA/US multimodal imaging-guided sonodynamic plaque neovascularization therapy. (**B**) Representative histopathological staining of plaque sections showing less plaque neovascularization and stable atherosclerotic plaque on day 28 after treatment of the advanced plaques in rabbits. Red arrows indicate abnormal adventitial neovessels. White arrows indicate intraplaque hemorrhage. (**A** and **B**) were reproduced with permission under the terms of the CC-BY license. Yao J, Yang Z, Huang L, et al. Low-Intensity focused ultrasound-responsive ferrite-encapsulated nanoparticles for atherosclerotic plaque neovascularization theranostics. *Adv Sci*. 2021;8(19):e2100850.[151]

therapeutic effects in patients with vulnerable atherosclerotic plaques.[136] Jiang et al conducted a phase-2, randomized, sham-controlled, double-blind clinical trial (NCT03457662) that enrolled 32 patients with symptomatic femoropopliteal AS. PET/CT confirmed that SDT prominently decreased the target-to-background ratio in the worst lesion by 0.53 on day 30 compared with control group. It also reduced the plaque area by 7.2%, improved local stenosis by 9.6%, and increased the score evaluating walking speed and physical function. Moreover, these improvements were maintained for up to 6 months, suggesting the great potential of SDT in clinical use to regress and stabilize plaque and improve the quality of life.[152] Another trial of DVDMS-SDT (NCT03382249) on carotid AS is still underway, and we are looking forward to see its treatment effect and safety problems.

The Challenge and Resolutions for Clinical Transition

Nanomaterial-based therapies have emerged as a promising approach for the treatment of AS, as they can be designed to target specific cells or tissues and deliver therapeutic agents directly to the site of AS plaques. However, the clinical translation of nanomaterial-based therapies for AS presents several challenges that should be overcome to ensure their safety and efficacy.

One of the main challenges of clinical transition for nanomaterial-based therapy for AS is to ensure their targeted delivery to the site of plaques. The design of nanomaterials can be optimized to achieve targeted delivery, but this requires a thorough understanding of the underlying mechanisms of AS and the specific cells and tissues involved in plaque formation. In this review, we have included many nanomaterials that are combined with specific antibody to target certain cells, such as macrophages or VSMCs more precisely, which is very promising in clinical use, especially precision medicine. Additionally, the pharmacokinetics and biodistribution of the nanomaterials must be carefully optimized to ensure that the therapeutic agents are delivered to the site of plaque formation while minimizing off-target effects. During design and synthesis of the materials, detrimental materials should be avoided or neutralized to minimize the risks, while more in vivo experiments have to be conducted to verify the good biocompatibility of materials in blood and tissues. Whether the materials will cause side effects is still the main concern before clinical application and should be clearly mentioned in the research.

Another challenge of clinical transition for nanomaterial-based therapy for AS is the evaluation of their safety and efficacy. Preclinical studies have shown promising results for nanomaterial-based therapies for AS, but it is important to

Table 1 Safety of Nanomaterials for AS Therapy

Treatment	Materials	Target	Animal	Dosage	Biocompatibility	Reference
PTT	Gold nanoparticles	–	ApoE-/- mice	0.4 μmol Au per g body weight	Large amounts of Au elements were found in reticuloendothelial system (RES) of spleen and liver. No significant organ damage and inflammatory lesions were found.	[47]
	Single-walled carbon nanotubes (SWNTs)	-	Mice	0.6 nmol/mouse	No observed significant acute or chronic toxicity with regard to clinical and laboratory parameters, histology, or survival in mice followed 3 to 5 months after injection.	[48]
	$CuCo_2S_4$	-	ApoE-/- mice	80 μg mL-1, 100 μL	No obvious toxicity to the major organs. No significant side effect on liver and kidney function.	[49]
	Cu_3BiS_3 nanocrystals	-	ApoE-/- mice	10 mg kg-1	No significant change in the shape and size of the cells. Cu3BiS3 nanocrystals mainly accumulate in the kidney and spleen after the intravenous administration. The content in these two organs gradually decreased over time, indicating that Cu3BiS3 nanocrystals were mainly degraded through these two organs.	[51]
	MoO_2 nanoclusters	-	ApoE-/- mice	80 ppm	The material mainly accumulate in the liver and spleen, which indicates that it was mainly degraded in these organs. No particle accumulation, obvious organ damage, or abnormal blood test results were noted due to local administration.	[50]
	CS-CNCs@Ce6/DS	Activated macrophages that express the type A scavenger receptor (SR-A)	ApoE-/- mice	-	No obvious tissue abnormalities. No clear toxicity to the major organs. No obvious hepatotoxicity or nephrotoxicity in mice. NPs accumulating in vivo are excreted in the urine. The nanoplatform caused no evident side effects on atherosclerotic mice and could be metabolized in vivo.	[53]

	CuS-TRPV1	Vascular smooth muscle cells (VSMCs)	ApoE-/- mice	10 mg kg−1	No noticeable organ damage.	[56]
	V-PPZ-NPs	Vascular endothelial cells (VECs)	Nude mice	5 mg mL−1	No significant weight change Major organs (heart, liver, spleen, lung and kidney) showed relatively normal histological structures.	[59]
	PFH@PLGA/MnFe(2)O(4)-Ram nanoparticles	Endothelial cells	New Zealand rabbits	50 mg	In SD rats, the levels of blood indices and histopathological aspects of the organs were almost unchanged. 30.33% of the UMFNPs (3 nm MnFe2O4) was excreted via the renal route and approximately 67.40% via the hepatobiliary route within 60 h. In plaque-bearing rabbits, on day 28 after PTT treatment, blood biochemical indices and weight were found unchanged compared with the baseline. There was negligible toxicity toward the main organs compared with the other groups.	[60]
	H-CuS@DMSN-N and H-CuS@DMSN-N=C-HA	CD44-positive inflammatory macrophages	New Zealand rabbits	3 mg mL-1	PT and FIB indexes showed no significant difference. APTT and TT values increased significantly. No obvious toxicity to liver or kidney. No significant histological toxicity to the major organs (heart, liver, spleen, lung, and kidney).	[55]
	Ag/Ag2S Janus beads (AAS JBs)	-	ApoE-/- mice	100 μL 250 μg mL-1	The material cause little production of pro-inflammatory cytokines. The blood indexes obtained from blood biochemistry and complete blood panel analysis show no abnormal change. No inflammation or damage is observed in major organs. The material mainly accumulates in the kidney and liver, thus, it was assumed to be excreted through these two organs.	[52]
	MJAMS/PTX/aV nanomotors	-	New Zealand rabbits	-	The material causes low hemolytic rates (<5%), which means no obvious damage to red blood cells (RBCs). No significant change in weight and major organs (heart, liver, spleen, lungs and kidneys).	[57]

(*Continued*)

https://doi.org/10.2147/IJN.S402678

Table 1 (Continued).

Treatment	Materials	Target	Animal	Dosage	Biocompatibility	Reference
	MMS/Au/PTX/VEGF/aV	VCAM-1 adhesion molecules on the surface of vascular endothelial cells	ApoE-/- mice	50 mg kg−1	During the entire treatment, no mice showed any abnormalities, and all mice maintained a slight weight gain. The materials were mainly distributed in the kidneys, indicating that the micromotors may be excluded from the metabolic organs. At the beginning (24 h) and the end (2 months) of treatment, the micromotors would not cause obvious main organ toxicity and blood toxicity in the mice.	[61]
	CD-LA-Au-aV	No	ApoE-/- mice	50 mg kg−1	The materials are almost completely cleared from the blood after 48 h. There is no abnormality or death in the mice during the whole treatment process, and the mice maintained slight weight gain. The materials did not cause toxicity in major organs and blood of mice at the starting (1d) and ending (60d) stages of treatment. Au element is found in the kidney, suggesting that the materials may be cleared in the metabolic organs.	[62]
	HA-HNSs	CD44+ cells	ApoE-/- mice	10 mg/kg	The half life was determined to be 2.71 h. HA-HNSs were partially metabolized in the liver and bound to monocytes and macrophages which were accumulated in the spleen. The hemolysis rate was less than 5%, suggesting the good hemocompatibility. The curves of mouse body weight showed no difference within 14 days after treatment. No systemic monocytes/macrophages decrease. There was no significant change in the liver and kidney function markers, as well as in the myocardial injury marker, echocardiogram, electrocardiogram and SpO2. No substantial tissue damage or inflammatory lesions in major organs were observed	[63]
	Silica–gold nanoparticles	-	Yucatan swine with inherited hyper-low-density lipoprotein (LDL) cholesterolemia and hypercholesterolemia and bearing mutant alleles for apolipoprotein B		The highest level of accumulation with NPs was directly in the studied plaques (> 900–1000 NPs/cm3; > 10 lg/mL), in the surrounding and neighboring healthy vascular tissues (400–600 units per cm3; 5.4 lg/mL), and in the liver and spleen, without signs of fibrosis or allergic responses. without any detrimental morphological dynamics.	[64–66]

PDT	PM-PAAO-UCNPs	-	ApoE-/- mice	15 mg/kg	The elimination half-life was 7.45 h for PM-PAAO-UCNPs. The reticuloendothelial system (RES) in liver and spleen, contained the most nanoparticles. No distinguishable injuries in major organs, and no obvious body weight change was observed. Levels of red blood cells, white blood cells, platelets, and hemoglobin were in normal ranges. There is little influence on liver and kidney functions.	[118]
	mTHPC-loaded Ben-PCL-mPEG micelles	-	Balb/c nude mice	5.0 and 0.6% mTHPC loading	Half-life times (t1/2 values): 1.5 hours. The materials was present in liver, spleen, kidney and lung in varying degrees after 4 hours of injection.	[110]
	TPZ/IR780@HSA-OPN	Overexpression of OPN in activated foamy macrophages	ApoE-/- mice	1mg/kg IR780	The materials had no distinct hemolytic activity in comparison with the control. No significant alteration on the levels of biochemical blood biomarkers, indicating no obvious damage to liver, renal, and cardiac function and little risk of diabetes mellitus. No overt tissue damage.	[115]
	FeCNPs	-	ApoE-/- mice	Low-dose (0.5 mg/kg CPPO), and high-dose (2 mg/kg CPPO) FeCNPs	The materials accumulated mainly in spleens and kidneys. The content of the materials in hearts, aortae, and livers at 48 hours decreased obviously from 24 hours.	[119]
SDT	PFP-HMME@PLGA/ $MnFe_2O_4$-ramucirumab nanoparticles (PHPMR NPs)	Mitochondria of rabbit aortic endothelial cells (RAECs)	New Zealand rabbits	1 mg mL−1, 50 mL, Fe + Mn: 269.7 mg L−1	No obvious changes were observed in the blood indexes or histopathological lesions in the organs. The rapid excretion of MnFe2O4 within 60 h is beneficial to minimize systematic toxicity. On day 28 after treatment, the changes in blood biochemical indices and weight fluctuations were negligible.	[151]

https://doi.org/10.2147/IJN.S402678

Table 2 Summary of Nanomaterials for Dynamic-Based AS Therapy

Field	Materials	Constitution	Radiation Dose for PTT and PTT; Ultrasound Frequency, Intensity/ Pressure, Time for SDT	Treatment Effect	Reference
PTT	Gold nanoparticles	–	808 nm; 2 W cm^{-2}; 10 min	Decreased the number of macrophages and the thickness of intima media.	[47]
	$CuCo_2S_4$	–	808 nm; 0.56 W cm^{-2}	Less macrophage infiltration. Significant reduction of the intima and media thickness.	[49]
	Cu_3BiS_3 nanocrystals	–	808 nm; 0.4 W cm^{-2}; 5 min	Less macrophage infiltration. Lower thickness of the intima/ media.	[51]
	MoO_2 nanoclusters	–	808 nm; 0.69 W cm^{-2}; 10 min	Inhibited carotid wall hyperplasia caused by inflammation.	[50]
	Silica–gold nanoparticles	Stable silica-gold NPs with 1,4,7,10,13,16,21, 24-octaazabicyclo[8.8.8] hexacosane (azacryptand)	821 nm; 35–44 W cm^{-2}; 7 min; for human	Destruction of a plaque with regression of atheroma.High safety with better rate of mortality, major adverse cardiovascular events and target lesion revascularization at the long-term follow-up if compare with stent	[64–66]
	CS-CNCs@Ce6/DS	Chitosan (CS) and Carbon nanocages (CNCs) formed chitosan-coated carbon nanocage (CS-CNC), chlorin e6 (Ce6) and dextran sulfate (DS)	808 nm; 1 W cm^{-2}; 10 min and 633 nm; 80 mW cm^{-2}; 10 min	Less SR-A expression, lower mRNA levels of pro-inflammatory markers in lesions, reduced proliferation and migration of SMCs and reduced lesion areas.	[53]
	CuS-TRPV1	CuS NP conjugated with a TRPV1 monoclonal antibody	980 nm; 5 W cm^{-2}; at the cardiac region for 30 cycles	Activated TRPV1. Reduced lesion areas.	[56]
	PFH@PLGA/MnFe(2)O(4)-Ram nanoparticles (NPs)	3 nm manganese ferrite (MnFe2O4) Perfluorohexane (PFH) Polylactic acid-glycolic acid (PLGA) Anti-VEGFR-2 antibody	808nm; 2 W cm^{-2}; 15 min	Reduced the number of macrophages, the percentage ratio of lipids, the HIF-1α score and increased collagen content. Reduced the inflammation level in the plaque. Resulted in more apoptotic neovessels with reduced hypoxic areas. Lumen area was increased and lesion area was decreased.	[60]

	H-CuS@DMSN-N and H-CuS@ DMSN-N=C-HA	Dendritic mesoporous silica nanoparticles (DMSN) Copper sulfide (CuS) Anticoagulant drug heparin (Hep) Oxidized hyaluronic acid (oxi-HA)	980 nm; 2.0 W cm^{-2}; 10 min	Ablated macrophages and thrombus.	[55]
	Ag/Ag2S Janus beads (AAS JBs)	Ag, Ag2S and polyvinylpyrrolidone (PVP)	808 nm; 0.7 W cm^{-2}; 5 min	Lower numbers of macrophages and lower thickness of intima.	[52]
	MJAMS/PTX/aV nanomotors	Aminated mesoporous silica (AMS) modified with platinum (Pt) was on one-side to form Janus AMS (JAMS). Modified with anti-proliferative drug PTX and anti-vascular cell adhesion molecule-1 (anti-VCAM-1) antibody. Wrapped with platelet membrane.	NIR laser; 2.0 W cm^{-2}; 10 min	Reduced hyperplasia area.	[57]
	MMS/Au/PTX/VEGF/aV	mesoporous-macroporous silica (MMS) Gold nanoparticles (Au NPs) Vascular endothelial growth factor (VEGF) Antiproliferative drug paclitaxel (PTX) anti-VCAM-1 polyclonal antibody (aV)	NIR laser; 2.5 W cm^{-2}; 10 min	Reduced formation of lipid plaques and lesion area.	[61]
	CD-LA-Au-aV	L-arginine (LA) β-cyclodextrin (β-CD), Au nanoparticles (Au NPs) 6-(mercaptohexyl) ferrocene (FcH) Anti-VCAM-1 monoclonal antibody (aV)	808 nm; 2.5 W cm^{-2}; 10 min	Reduced plaque area. Decreased index of LDL and increased index of HDL in blood.	[62]
	bTiO2-HA-p	Black TiO2 (bTiO2) nanoparticles Hyaluronan (HA) Porphine	808 nm; 1 W cm^{-2}; 10 min; in vitro	Reduced the intracellular lipid burden without inducing evidently apoptosis or necrosis.	[58]
	HA-HNSs	Hyaluronic acid (HA)- and PEG-modified CuS/TiO2 heterostructure nanosheets	1064 nm; 0.8 W cm-2; 10 min Ultrasound intensity at 0.5 W cm^{-2}; 10 min	Lower ratio of the lesion area and decreased content of intraplaque macrophage and proinflammatory cytokines.	[63]

(*Continued*)

https://doi.org/10.2147/IJN.S402678

Table 2 (Continued).

Field	Materials	Constitution	Radiation Dose for PTT and PTT; Ultrasound Frequency, Intensity/ Pressure, Time for SDT	Treatment Effect	Reference
PDT	Hematoporphyrin derivative (HpD)	-	636 nm; total fluence of 27 mJ cm^{-2}; 10min	Induced cell necrosis in intimal and media and inhibited initial hyperplasia.	[69–72]
	dihematoporphyrin ether (photofrin II)	-	632 nm; 150 mW cm^{-2}; 30 J cm^{-2} (total output); for human	Decreased intimal thickness and enlarged luminal diameter. Reduced lipid content in plaque. In patients no adverse events such as photodermatosis, or myocardial ischemia had occurred. No in-stent restenosis was observed.	[73–79,120]
	ALA-PPIX	-	635 nm; a total dose of 50 J cm^{-2}; 500 and 1500 s, and 200 and 390 s for the iliacs and coronaries, respectively in human	Decreased number of VSMCs in the media and inhibited intimal hyperplasia. Increased maximal lumen diameter. Patients tolerated the procedure well without adverse complications or death. All were rendered asymptomatic throughout the study interval. All vessels remained patent and no lesion attained the duplex definition of restenosis.	[84–89]
	Indocyanine green (ICG)	-	780 nm; 4 J cm^{-2}	Reduced arterial wall thickness.	[93]
	e6	-	670 nm; 72.6 mW cm^{-2} (dose rate); 4.4 J cm^{-2} (irradiation dose)	Damaged elastic fiber network in plaque. Dissociated ester bonds of cholesterol esters. Attenuated cathepsin B-related signal.Decreased macrophage infiltration by inducing apoptosis without affecting plaque size or number of VSMCs.	[94–98]
	Activity-Based Probed (PS-qABP)	Photosensitizer (bChlo) and quencher (QC-1) attached to GB111-NH2 scaffold	760nm, 50mW, 20min	Reduced immune cell content without affecting VSMC and collagen contents.	[99]
	Motexafin lutetium	-	730±6 nm; 100 to 400 J/cm-fiber; 12min; in human	Increased number of apoptotic cells. Therapy was well tolerated. No deleterious vascular effects. Several secondary end points suggested a favorable therapeutic effect.	[100–102,121,122]
	PH-1126	9-desoxo-9 (R,S) -hydroxy-10 (R) -N,N-dimethylaminoethyl-pheophorbide-a	647 nm; 100 J cm^{-2} (irradiation dose)	Endothelial layer of the lesion was ruptured and numerous teardrop-shaped cells resembled foam cells were observed.	[103]

	Pyropheophorbide-alpha methyl ester (MPPa)	-	630 nm; 30 mW cm^{-2}; for the indicated time; in vitro	Induced RAW264.7 cell apoptosis. Decreased secretion of inflammatory cytokines.	[104]
	Curcumin (CUR)	-	425 nm; 40 mW cm^{-2}; 6 hours	Promoted autophagy and inhibited differentiation of VSMCs. Reduced cell migration and lipid droplet numbers in cells.	[106]
	ALA dendrimers	-	400–700 nm; 0.5 mW cm^{-2} (power density); 0.15 or 0.6 J cm^{-2} (irradiation dose); in vitro	High selectivity on macrophages as compared to endothelial cells. Induced cell death.	[108,109]
	DS-Ce6	Dextran sulfate(DS) and Ce6	670 nm; 1 W cm^{-2} (fluence rate); 150 seconds	Reduced plaque burden and inflammation. Increased apoptotic macrophages and induced autophagy and efferocytosis.	[112]
	Glu/Ce6 nanocomplexes	Glucan and Chlorin e6	670 nm; 50 mW cm^{-2}; 1 min	Induced significant membrane damage and apoptosis of foam cells.	[113]
	UCNPs-Ce6	Chlorin e6 (Ce6), onto silica-coated upconversion nanoparticles	980nm; 1.0 W cm^{-2}; 60s; in vitro	Resulted in apoptosis of THP-1 macrophages and enhanced the cholesterol efflux and the induction of autophagy.	[114,116,117]
	PM-PAAO-UCNPs	Incorporating UCNPs and Ce6 into polyacrylic acid-n-octylamine (PAAO) micelles, followed by PM coating	980 nm; 10 mW cm^{-2}; 30 min	Alleviated plaque progression. Induced foam cell apoptosis and ameliorated inflammation. Triggered lipid efflux from foam cells. Increased the expression of cell marker of VSMCs.	[118]
	TPZ/IR780@HSA-OPN	Human serum albumin (HSA) conjugated with a high affinity-peptide targeting osteopontin (OPN) and encapsulated with photosensitizer IR780 and hypoxia-activatable tirapazamine (TPZ)	808 nm; 1.5 W cm^{-2}; 3 min	Resulted in plaque ablation and amplified hypoxia. Suppressed foamy macrophages. Reduced plaque area and degree of carotid artery stenosis.	[115]
	FeCNPs	Monomethoxypolyethylene glycol-block-poly(L-lysine) modified with Ce6 and 3,4-DA (mPEG-Plys -[DA-Ce6]) was synthesized and self-assembled with CPPO. To improve stability, Fe3+ was introduced to coordinate with catechol groups	-	Eliminated macrophages and prevented progression of plaque. Reduced plaque size and thickness	[119]

(*Continued*)

https://doi.org/10.2147/IJN.S402678

Table 2 (Continued).

Field	Materials	Constitution	Radiation Dose for PTT and PTT; Ultrasound Frequency, Intensity/ Pressure, Time for SDT	Treatment Effect	Reference
SDT	PpIX	-	1.0 MHz; 0.5 W cm^{-2}; 5 min; in vitro	Induced both apoptosis and necrosis of THP-1 macrophages	[15,126]
	5-ALA		1.0 MHz; 1.5W cm^{-2} for rabbits and 0.8 W cm^{-2} for mice;15min	Decreased size of the atherosclerotic plaque and enlarged lumen. Reduction in lesional macrophages and lipids.	[17,127–135]
	Sinoporphyrin sodium (DVDM)	-	1.0 MHz; 1.5 W cm^{-2} for rabbits, 0.8 W cm^{-2} for mice; 15 min For human: 2.1 W cm^{-2} in the common femoral artery and superficial femoral artery, and 1.8 W cm^{-2} in popliteal artery	Reduced arterial inflammation and angiogenesis. Alleviated iron retention in hemorrhagic plaques. Enhanced macrophage efferocytosis. inhibited the progression of atherosclerosis, reduced the macrophage content, and increased the smooth muscle cell content.	[136–138,152]
	Emodin	-	0.86 MHz; 0.44 W cm^{-2}; 15 min; in vitro	Decreased cell viability and increased apoptotic and necrotic cells.	[139]
	Hydroxyl acetylated curcumin (HAC)	-	1.0 MHz; 0.5 W cm^{-2}; for indicated time; in vitro	Induced apoptosis of macrophages and autophagy with decrease in the lipid uptake.	[1,41,142]
	Curcumin nanosuspensions (Cur-ns)	Polyvinylpyrrolidone (PVPK30), sodium dodecyl sulfate (SDS) and curcumin	1.0 MHz; 0.4 W cm^{-2}; 15 minutes	Reduced the level of total cholesterol (TC) and low density lipoprotein (LDL). Promoted the transformation from M1 to M2 macrophages. Relieved atherosclerosis syndrome.	[150]
	ALA:AuNPs	Methyl ester of aminolevulinic acid (MALA), gold nanoparticles (MALA: AuNPs) and polyethylene glycol (PEG)	1 MHz; 1 W cm^{-2}; 2 minutes	Culminated with total macrophage reduction	[1,48,149]
	PFP-HMME@PLGA/ $MnFe_2O_4$-ramucirumab nanoparticles (PHPMR NPs)	Manganese ferrite (MnFe2O4), hematoporphyrin monomethyl ether (HMME), perfluoropentane (PFP), polylactic acid-glycolic acid (PLGA) shells and anti-VEGFR-2 antibody.	1 MHz; 1.5 Wcm^{-2}; 15 min	Induced apoptosis in neovessel endothelial cells and improved hypoxia. Reduced the density of neovessels, subsequently inhibiting intraplaque hemorrhage and inflammation and stabilizing the plaque.	[151]

evaluate their safety and efficacy in clinical trials (Table 1). The clinical trials should be carefully designed to ensure that they meet all safety and efficacy standards and that the outcomes are clinically meaningful.

To overcome these challenges, several resolution suggestions have been proposed. Thorough understanding of the underlying mechanisms of AS and the specific cells and tissues involved in plaque formation have to be developed to inform the design of nanomaterials for targeted delivery. The pharmacokinetics and biodistribution of nanomaterials should be optimized to achieve targeted delivery to the site of plaque formation. More well-designed clinical trials are necessary to evaluate the safety and efficacy of nanomaterial-based therapies for AS, especially random clinical trials (RCT), which should include larger sample size than those we mentioned in the articles. Researchers need to engage with regulatory agencies to ensure that the therapies meet all safety and efficacy standards. For instance, most photosensitizers will result in skin photosensitivity, and this side effect should be clearly investigated. Meanwhile, collaboration with stakeholders including patients and healthcare providers is recommended to ensure that the benefits and risks of nanomaterial-based therapies for AS are clearly communicated.

In summary, the clinical transition of nanomaterial-based therapies for AS presents several challenges that must be overcome to ensure their safety and efficacy. However, with careful design and optimization, rigorous preclinical and clinical testing, and close collaboration with regulatory agencies and stakeholders, nanomaterial-based therapies have the potential to transform the treatment of AS and improve patient outcomes.

Conclusion and Prospects

In this review, we systematically introduced the basic physical principles and biological mechanisms associated with ROS-derived therapeutic strategy, and summarized the recent advances in PDT, PTT, and SDT treatment strategies based on AS (Table 2). The creation of sensitizers for PTT, PDT, and SDT requires the design and development of more organic and inorganic sensitizer small molecules, a reliance on good nanomaterial science platforms, and the establishment of more efficient and rigorous treatment assessment methods.

With the development of nanotechnology and the demand for effective treatments for AS, a variety of novel nanomaterials combined with conversion-based characteristics have been discovered and applied in animal models. However, the clinical transition of these nanomaterials poses some challenges.

The first challenge is that the inherent AS microenvironment (such as its acidic nature) may weaken PTT, PDT, and SDT treatment effects. The development of atherosclerotic plaque microenvironment-responsive multifunctional sonosensitizers is highly effective. In addition, biomolecules such as proteins, lipids, and nutrient molecules are abundantly distributed in the AS microenvironment. These biomolecules can absorb onto the surface of the NPs to form a layer called the “biomolecule corona”. For example, the biomolecule corona may alter their biodistribution in the body and modulate their interaction with the immune system.[153] Therefore, it is necessary to consider the interactions between NPs and biological molecules to understand the behaviors in AS microenvironments.

The second challenge is, as the recent research has revealed, the targeting abilities of sonosensitizers or photosensitizers are very low. To improve the AS targeting ability, some excellent targeting ligands, such as cell membrane coating, specific antibodies and protein modification, and extracellular vesicle loading, have been developed. Targeting therapy based on nanotechnology has brought new possibilities for the individualized precision treatment of atherosclerotic plaques.

Finally, owing to the complexity of AS, nano-dynamic therapy methods usually kill plaque foam cells. A synergistic combination of multiple treatments, such as immunotherapy, will greatly improve the therapeutic efficacy of AS. With regard to practical applications, the development of a complete AS therapy (including PDT and other therapies) will lead to better clinical outcomes and give patients hope.

Acknowledgments

This work was funded by the National Natural Science Foundation of China (No.81972444) and the National High Level Hospital Clinical Research Funding (No.2022-PUMCH-A-231).

Disclosure

The authors declare no conflicts of interest in this work.

References

1. Cardiovascular diseases (CVDs). Available from: https://www.who.int/en/news-room/fact-sheets/detail/cardiovascular-diseases-(cvds). Accessed November, 2022.
2. Bäck M, Yurdagul A, Tabas I, Öörni K, Kovanen PT. Inflammation and its resolution in atherosclerosis: mediators and therapeutic opportunities. *Nat Rev Cardiol*. 2019;16(7):389–406. doi:10.1038/s41569-019-0169-2
3. Bentzon JF, Otsuka F, Virmani R, Falk E. Mechanisms of plaque formation and rupture. *Circ Res*. 2014;114(12):1852–1866. doi:10.1161/CIRCRESAHA.114.302721
4. Tian J, Ren X, Vergallo R, et al. Distinct morphological features of ruptured culprit plaque for acute coronary events compared to those with silent rupture and thin-cap fibroatheroma: a combined optical coherence tomography and intravascular ultrasound study. *J Am Coll Cardiol*. 2014;63(21):2209–2216. doi:10.1016/j.jacc.2014.01.061
5. T J, D H, T C, et al. Prevalence and characteristics of TCFA and degree of coronary artery stenosis: an OCT, IVUS, and angiographic study. *J Am Coll Cardiol*. 2014;64(7):672–680. doi:10.1016/j.jacc.2014.05.052
6. Ascer E, Bertolami MC, Venturinelli ML, et al. Atorvastatin reduces proinflammatory markers in hypercholesterolemic patients. *Atherosclerosis*. 2004;177(1):161–166. doi:10.1016/j.atherosclerosis.2004.07.003
7. Lobatto ME, Fuster V, Fayad ZA, Mulder WJM. Perspectives and opportunities for nanomedicine in the management of atherosclerosis. *Nat Rev Drug Discov*. 2011;10(11):835–852. doi:10.1038/nrd3578
8. Gisterå A, Hansson GK. The immunology of atherosclerosis. *Nat Rev Nephrol*. 2017;13(6):368–380. doi:10.1038/nrneph.2017.51
9. X-H Y, Zhang D-W, Zheng X-L, Tang C-K. Cholesterol transport system: an integrated cholesterol transport model involved in atherosclerosis. *Prog Lipid Res*. 2019;73:65–91. doi:10.1016/j.plipres.2018.12.002
10. Zhai M, Gong S, Luan P, et al. Extracellular traps from activated vascular smooth muscle cells drive the progression of atherosclerosis. *Nat Commun*. 2022;13(1):7500. doi:10.1038/s41467-022-35330-1
11. Lin X, Ouyang S, Zhi C, et al. Focus on ferroptosis, pyroptosis, apoptosis and autophagy of vascular endothelial cells to the strategic targets for the treatment of atherosclerosis. *Arch Biochem Biophys*. 2022;715:109098. doi:10.1016/j.abb.2021.109098
12. Luo Y, Li J, Huang C, Wang X, Long D, Cao Y. Graphene oxide links alterations of anti-viral signaling pathways with lipid metabolism via suppressing TLR3 in vascular smooth muscle cells. *Mol Omics*. 2022;18(8):779–790. doi:10.1039/d2mo00086e
13. Ochsner M. Photophysical and photobiological processes in the photodynamic therapy of tumours. *J Photochem Photobiol B*. 1997;39(1):1–18. doi:10.1016/S1011-1344(96)07428-3
14. Castano AP, Demidova TN, Hamblin MR. Mechanisms in photodynamic therapy: part one-photosensitizers, photochemistry and cellular localization. *Photodiagnosis Photodyn Ther*. 2004;1(4):279–293. doi:10.1016/S1572-1000(05)00007-4
15. Guo S, Sun X, Cheng J, et al. Apoptosis of THP-1 macrophages induced by protoporphyrin IX-mediated sonodynamic therapy. *Int J Nanomedicine*. 2013;8:2239–2246. doi:10.2147/IJN.S43717
16. Dan J, Sun X, Li W, et al. 5-aminolevulinic acid-mediated sonodynamic therapy promotes phenotypic switching from dedifferentiated to differentiated phenotype via reactive oxygen species and p38 mitogen-activated protein kinase in vascular smooth muscle cells. *Ultrasound Med Biol*. 2015;41(6):1681–1689. doi:10.1016/j.ultrasmedbio.2014.12.664
17. Tian F, Yao J, Yan M, et al. 5-Aminolevulinic Acid-Mediated Sonodynamic Therapy Inhibits RIPK1/RIPK3-Dependent Necroptosis in THP-1-Derived Foam Cells. *Sci Rep*. 2016;6:21992. doi:10.1038/srep21992
18. Yang Y, Liu Y, Chen X, et al. 5-aminolevulinic acid-mediated sonodynamic therapy alleviates atherosclerosis via enhancing efferocytosis and facilitating a shift in the Th1/Th2 balance toward Th2 polarization. *Cell Physiol Biochem*. 2018;47(1):83–96. doi:10.1159/000489751
19. Crum LA, Roy RA. Sonoluminescence. *Science*. 1994;266(5183):233–234. doi:10.1126/science.266.5183.233
20. Lohse D. Sonoluminescence: cavitation hots up. *Nature*. 2005;434(7029):33–34. doi:10.1038/434033a
21. Yasui K, Tuziuti T, Lee J, Kozuka T, Towata A, Iida Y. Numerical simulations of acoustic cavitation noise with the temporal fluctuation in the number of bubbles. *Ultrason Sonochem*. 2010;17(2):460–472. doi:10.1016/j.ultsonch.2009.08.014
22. Suslick KS. Sonochemistry. *Science*. 1990;247(4949):1439–1445. doi:10.1126/science.247.4949.1439
23. Huber PE, Debus J. Tumor cytotoxicity in vivo and radical formation in vitro depend on the shock wave-induced cavitation dose. *Radiat Res*. 2001;156(3):301–309. doi:10.1667/0033-7587(2001)156[0301:TCIVAR]2.0.CO;2
24. Villeneuve L, Alberti L, Steghens JP, Lancelin JM, Mestas JL. Assay of hydroxyl radicals generated by focused ultrasound. *Ultrason Sonochem*. 2009;16(3):339–344. doi:10.1016/j.ultsonch.2008.09.007
25. Xu H, Sun X, Yao J, et al. The decomposition of protoporphyrin IX by ultrasound is dependent on the generation of hydroxyl radicals. *Ultrason Sonochem*. 2015;27:623–630. doi:10.1016/j.ultsonch.2015.04.024
26. Pankaj. Aqueous Inorganic Sonochemistry. In: Ashokkumar M, editor. *Theoretical and Experimental Sonochemistry Involving Inorganic Systems*. Berlin: Springer-Verlag; 2011:213–271.
27. Yasui K. Multibubble sonoluminescence from a theoretical perspective. *Molecules*. 2021;26(15):4624. doi:10.3390/molecules26154624
28. Kondo T, Krishna CM, Riesz P. Pyrolysis radicals formed by ultrasound in aqueous solutions of nucleotides: a spin trapping study. *Int J Radiat Biol*. 1990;57(1):23–33. doi:10.1080/09553009014550311
29. Riesz P, Kondo T. Free radical formation induced by ultrasound and its biological implications. *Free Radic Biol Med*. 1992;13(3):247–270. doi:10.1016/0891-5849(92)90021-8
30. Torii T, Yasui K, Yasuda K, et al. Generation and consumption rates of OH radicals in sonochemical reactions. *Res Chem Intermed*. 2004;30(7):713–721. doi:10.1163/1568567041856918
31. Yasui K, Tuziuti T, Kozuka T, Towata A, Iida Y. Relationship between the bubble temperature and main oxidant created inside an air bubble under ultrasound. *J Chem Phys*. 2007;127(15):154502. doi:10.1063/1.2790420

32. Yasui K, Tuziuti T, Iida Y, Mitome H. Theoretical study of the ambient-pressure dependence of sonochemical reactions. *J Chem Phys*. 2003;119(1):346–356. doi:10.1063/1.1576375
33. Yusof NSM, Anandan S, Sivashanmugam P, Flores EMM, Ashokkumar M. A correlation between cavitation bubble temperature, sonoluminescence and interfacial chemistry - A mini review. *Ultrason Sonochem*. 2022;85:105988. doi:10.1016/j.ultsonch.2022.105988
34. Winyard PG, Moody CJ, Jacob C. Oxidative activation of antioxidant defence. *Trends Biochem Sci*. 2005;30(8):453–461. doi:10.1016/j.tibs.2005.06.001
35. Nowak WN, Deng J, Ruan XZ, Xu Q. Reactive oxygen species generation and atherosclerosis. *Arterioscler Thromb Vasc Biol*. 2017;37(5):e41–e52. doi:10.1161/ATVBAHA.117.309228
36. Moloney JN, Cotter TG. ROS signalling in the biology of cancer. *Semin Cell Dev Biol*. 2018;80:50–64.
37. Zhao Y, Zhao B. Oxidative stress and the pathogenesis of Alzheimer's disease. *Oxid Med Cell Longev*. 2013;2013:316523. doi:10.1155/2013/316523
38. Bayir S, Barras A, Boukherroub R, et al. Mesoporous silica nanoparticles in recent photodynamic therapy applications. *Photochem Photobiol Sci*. 2018;17(11):1651–1674. doi:10.1039/c8pp00143j
39. Yu BP. Cellular defenses against damage from reactive oxygen species. *Physiol Rev*. 1994;74(1):139–162. doi:10.1152/physrev.1994.74.1.139
40. Forrester SJ, Kikuchi DS, Hernandes MS, Xu Q, Griendling KK. Reactive oxygen species in metabolic and inflammatory signaling. *Circ Res*. 2018;122(6):877–902. doi:10.1161/CIRCRESAHA.117.311401
41. Fiers W, Beyaert R, Declercq W, Vandenabeele P. More than one way to die: apoptosis, necrosis and reactive oxygen damage. *Oncogene*. 1999;18(54):7719–7730. doi:10.1038/sj.onc.1203249
42. Scherz-Shouval R, Elazar Z. Regulation of autophagy by ROS: physiology and pathology. *Trends Biochem Sci*. 2011;36(1):30–38. doi:10.1016/j.tibs.2010.07.007
43. Aprotosoaie AC, Costache A-D, Costache -I-I. Therapeutic strategies and chemoprevention of atherosclerosis: what do we know and where do we go? *Pharmaceutics*. 2022;14(4):722. doi:10.3390/pharmaceutics14040722
44. Dai T, He W, Yao C, et al. Applications of inorganic nanoparticles in the diagnosis and therapy of atherosclerosis. *Biomater Sci*. 2020;8(14):3784–3799. doi:10.1039/D0BM00196A
45. Lukianova-Hleb EY, Mrochek AG, Lapotko DO. Method for disruption and re-canalization of atherosclerotic plaques in coronary vessels with photothermal bubbles generated around gold nanoparticles. *Lasers Surg Med*. 2009;41(3):240–247. doi:10.1002/lsm.20749
46. Kosuge H, Nakamura M, Oyane A, et al. Potential of gold nanoparticles for noninvasive imaging and therapy for vascular inflammation. *Mol Imaging Biol*. 2021;24:692–699. doi:10.1007/s11307-021-01654-5
47. Qin J, Peng Z, Li B, et al. Gold nanorods as a theranostic platform for in vitro and in vivo imaging and photothermal therapy of inflammatory macrophages. *Nanoscale*. 2015;7(33):13991–14001. doi:10.1039/C5NR02521D
48. Kosuge H, Sherlock SP, Kitagawa T, et al. Near infrared imaging and photothermal ablation of vascular inflammation using single-walled carbon nanotubes. *J Am Heart Assoc*. 2012;1(6):e002568. doi:10.1161/jaha.112.002568
49. Zhang X, Liu J, Yang X, et al. CuCo2S4 nanocrystals as a nanoplatform for photothermal therapy of arterial inflammation. *Nanoscale*. 2019;11(19):9733–9742. doi:10.1039/C9NR00772E
50. Wang X, Wu X, Qin J, et al. Differential phagocytosis-based photothermal ablation of inflammatory macrophages in atherosclerotic disease. *ACS Appl Mater Interfaces*. 2019;11(44):41009–41018. doi:10.1021/acsami.9b12258
51. Lu R, Zhu J, Yu C, Nie Z, Gao Y. Cu3BiS3 nanocrystals as efficient nanoplatforms for CT imaging guided photothermal therapy of arterial inflammation. *Front Bioeng Biotechnol*. 2020;8:981. doi:10.3389/fbioe.2020.00981
52. Peng X, Liu J, Li B, et al. Janus Ag/Ag(2)S beads as efficient photothermal agents for the eradication of inflammation and artery stenosis. *Nanoscale*. 2019;11(42):20324–20332. doi:10.1039/c9nr04804a
53. Liu J, Zhou B, Guo Y, et al. SR-A-targeted nanoplatform for sequential photothermal/photodynamic ablation of activated macrophages to alleviate atherosclerosis. *ACS Appl Mater Interfaces*. 2021;2021:1.
54. Oh B, Lee CH. Development of Man-rGO for targeted eradication of macrophage ablation. *Mol Pharm*. 2015;12(9):3226–3236. doi:10.1021/acs.molpharmaceut.5b00181
55. Liu S, Zhao Y, Shen M, et al. Hyaluronic acid targeted and pH-responsive multifunctional nanoparticles for chemo-photothermal synergistic therapy of atherosclerosis. *J Mater Chem B*. 2022;10(4):562–570.
56. Gao W, Sun Y, Cai M, et al. Copper sulfide nanoparticles as a photothermal switch for TRPV1 signaling to attenuate atherosclerosis. *Nat Commun*. 2018;9(1):231. doi:10.1038/s41467-017-02657-z
57. Huang Y, Li T, Gao W, et al. Platelet-derived nanomotor coated balloon for atherosclerosis combination therapy. *J Mater Chem B*. 2020;8(26):5765–5775. doi:10.1039/D0TB00789G
58. Dai T, He W, Tu S, et al. Black TiO(2) nanoprobe-mediated mild phototherapy reduces intracellular lipid levels in atherosclerotic foam cells via cholesterol regulation pathways instead of apoptosis. *Bioact Mater*. 2022;17:18–28. doi:10.1016/j.bioactmat.2022.01.013
59. Chen YL, Liu FQ, Guo Y, et al. PA/US dual-modality imaging to guide VEGFR-2 targeted photothermal therapy using ZnPc-/PFH-loaded polymeric nanoparticles. *Biomater Sci*. 2018;6(8):2130–2143. doi:10.1039/c8bm00213d
60. Yang Z, Yao J, Wang J, et al. Ferrite-encapsulated nanoparticles with stable photothermal performance for multimodal imaging-guided atherosclerotic plaque neovascularization therapy. *Biomater Sci*. 2021;9(16):5652–5664. doi:10.1039/d1bm00343g
61. Li X, Wu R, Chen H, et al. Near-infrared light-driven multifunctional tubular micromotors for treatment of atherosclerosis. *ACS Appl Mater Interfaces*. 2021;13(26):30930–30940. doi:10.1021/acsami.1c03600
62. Wu Z, Wu R, Li X, et al. Multi-pathway microenvironment regulation for atherosclerosis therapy based on beta-cyclodextrin/L-arginine/au nanomotors with dual-mode propulsion. *Small*. 2022;18(9):e2104120. doi:10.1002/smll.202104120
63. Cao Z, Yuan G, Zeng L, et al. Macrophage-targeted sonodynamic/photothermal synergistic therapy for preventing atherosclerotic plaque progression using CuS/TiO heterostructured nanosheets. *ACS Nano*. 2022;16(7):10608–10622. doi:10.1021/acsnano.2c02177
64. Kharlamov AN, Gabinsky JL. Plasmonic photothermic and stem cell therapy of atherosclerotic plaque as a novel nanotool for angioplasty and artery remodeling. *Rejuvenation Res*. 2012;15(2):222–230. doi:10.1089/rej.2011.1305
65. Kharlamov AN, Tyurnina AE, Veselova VS, Kovtun OP, Shur VY, Gabinsky JL. Silica-gold nanoparticles for atheroprotective management of plaques: results of the NANOM-FIM trial. *Nanoscale*. 2015;7(17):8003–8015. doi:10.1039/c5nr01050k

66. Kharlamov AN, Feinstein JA, Cramer JA, Boothroyd JA, Shishkina EV, Shur V. Plasmonic photothermal therapy of atherosclerosis with nanoparticles: long-term outcomes and safety in NANOM-FIM trial. *Future Cardiol*. 2017;13(4):345–363. doi:10.2217/fca-2017-0009
67. Rockson SG, Lorenz DP, Cheong WF, Woodburn KW. Photoangioplasty: an emerging clinical cardiovascular role for photodynamic therapy. *Circulation*. 2000;102(5):591–596. doi:10.1161/01.cir.102.5.591
68. Kou J, Dou D, Yang L. Porphyrin photosensitizers in photodynamic therapy and its applications. *Oncotarget*. 2017;8(46):81591–81603. doi:10.18632/oncotarget.20189
69. Spears JR, Serur J, Shropshire D, Paulin S. Fluorescence of experimental atheromatous plaques with hematoporphyrin derivative. *J Clin Invest*. 1983;71(2):395–399. doi:10.1172/JCI110782
70. Litvack F, Grundfest WS, Forrester JS, et al. Effects of hematoporphyrin derivative and photodynamic therapy on atherosclerotic rabbits. *Am J Cardiol*. 1985;56(10):667–671. doi:10.1016/0002-9149(85)91032-x
71. Usui M, Asahara T, Naitoh Y, Katoh T, Ibukiyama C. Photodynamic therapy for the prevention of intimal hyperplasia in balloon-injured rabbit arteries. *Jpn Circ J*. 1999;63(5):387–393. doi:10.1253/jcj.63.387
72. Gonschior P, Erdemci A, Gerheuser F, et al. [Selective hematoporphyrin derivative (HMD) application in arterial vessels using a porous balloon catheter results in equivalent levels as compared to high-dose systemic administration]. *Z Kardiol*. 1991;80(12):738–745. German.
73. Neave V, Giannotta S, Hyman S, Schneider J. Hematoporphyrin uptake in atherosclerotic plaques: therapeutic potentials. *Neurosurgery*. 1988;23(3):307–312. doi:10.1227/00006123-198809000-00004
74. Dartsch PC, Ischinger T, Betz E. Responses of cultured smooth muscle cells from human nonatherosclerotic arteries and primary stenosing lesions after photoradiation: implications for photodynamic therapy of vascular stenoses. *J Am Coll Cardiol*. 1990;15(7):1545–1550. doi:10.1016/0735-1097(90)92824-l
75. Dartsch PC, Coppenrath E, Coppenrath K, Ischinger T. Photodynamic therapy of vascular stenosis: results from cell culture studies on human endothelial cells. *Coron Artery Dis*. 1993;4(2):207–213. doi:10.1097/00019501-199302000-00012
76. Tang G, Hyman S, Schneider JH Jr, Giannotta SL. Application of photodynamic therapy to the treatment of atherosclerotic plaques. *Neurosurgery*. 1993;32(3):438–443. doi:10.1227/00006123-199303000-00016
77. Hsiang YN, Crespo MT, Machan LS, Bower RD, Todd ME. Photodynamic therapy for atherosclerotic stenoses in Yucatan miniswine. *Can J Surg*. 1994;37(2):148–152.
78. Vincent GM, Mackie RW, Orme E, Fox J, Johnson M. In vivo photosensitizer-enhanced laser angioplasty in atherosclerotic Yucatan miniswine. *J Clin Laser Med Surg*. 1990;8(3):59–61. doi:10.1089/clm.1990.8.59
79. Amemiya T, Nakajima H, Katoh T, Rakue H, Miyagi M, Ibukiyama C. Photodynamic therapy of atherosclerosis using YAG-OPO laser and Porfimer sodium, and comparison with using argon-dye laser. *Jpn Circ J*. 1999;63(4):288–295. doi:10.1253/jcj.63.288
80. Hsiang YN, Crespo MT, Richter AM, Jain AK, Fragoso M, Levy JG. In vitro and in vivo uptake of benzoporphyrin derivative into human and miniswine atherosclerotic plaque. *Photochem Photobiol*. 1993;57(4):670–674. doi:10.1111/j.1751-1097.1993.tb02935.x
81. Allison BA, Crespo MT, Jain AK, Richter AM, Hsiang YN, Levy JG. Delivery of benzoporphyrin derivative, a photosensitizer, into atherosclerotic plaque of Watanabe heritable hyperlipidemic rabbits and balloon-injured New Zealand rabbits. *Photochem Photobiol*. 1997;65(5):877–883. doi:10.1111/j.1751-1097.1997.tb01938.x
82. Jain M, Zellweger M, Frobert A, et al. Intra-arterial drug and light delivery for photodynamic therapy using visudyne®: implication for atherosclerotic plaque treatment. *Front Physiol*. 2016;7:400. doi:10.3389/fphys.2016.00400
83. Cheng J, Liang H, Li Q, et al. Hematoporphyrin monomethyl ether-mediated photodynamic effects on THP-1 cell-derived macrophages. *J Photochem Photobiol B*. 2010;101(1):9–15. doi:10.1016/j.jphotobiol.2010.06.005
84. Pai M, Jamal W, Mosse A, Bishop C, Bown S, McEwan J. Inhibition of in-stent restenosis in rabbit iliac arteries with photodynamic therapy. *Eur J Vasc Endovasc Surg*. 2005;30(6):573–581. doi:10.1016/j.ejvs.2005.07.003
85. Gabeler EEE, van Hillegersberg R, Statius van Eps RG, Sluiter W, Mulder P, van Urk H. Endovascular photodynamic therapy with aminolaevulinic acid prevents balloon induced intimal hyperplasia and constrictive remodelling. *Eur J Vasc Endovasc Surg*. 2002;24(4):322–331. doi:10.1053/ejvs.2002.1723
86. Jenkins MP, Buonaccorsi G, MacRobert A, Bishop CC, Bown SG, McEwan JR. Intra-arterial photodynamic therapy using 5-ALA in a swine model. *Eur J Vasc Endovasc Surg*. 1998;16(4):284–291. doi:10.1016/S1078-5884(98)80047-6
87. Jenkins MP, Buonaccorsi GA, Mansfield R, Bishop CC, Bown SG, McEwan JR. Reduction in the response to coronary and iliac artery injury with photodynamic therapy using 5-aminolaevulinic acid. *Cardiovasc Res*. 2000;45(2):478–485. doi:10.1016/S0008-6363(99)00352-1
88. Jenkins GAB MP, Raphael M, Nyamekye I, McEwan JR, Bown SG, Bishop CCR. Clinical study of adjuvant photodynamic therapy to reduce restenosis following femoral angioplasty. *Br J Surg*. 1999;86(10):1258–1263. doi:10.1046/j.1365-2168.1999.01247.x
89. Herman MA, Webber J, Fromm D, Kessel D. Hemodynamic effects of 5-aminolevulinic acid in humans. *Biology*. 1998;43(1):61–65. doi:10.1016/S1011-1344(98)00086-4
90. Eldar M, Yerushalmi Y, Kessler E, et al. Preferential uptake of a water-soluble phthalocyanine by atherosclerotic plaques in rabbits. *Atherosclerosis*. 1990;84(2–3):135–139. doi:10.1016/0021-9150(90)90083-u
91. Dartsch PC, Wunderlich K, Ben-Hur E. Aluminium phthalocyanines-induced photolysis of human vascular wall cells in culture and the effect of fluoride on photodynamic action. *Coron Artery Dis*. 1994;5(10):851–855.
92. de Vries HE, Moor AC, Dubbelman TM, van Berkel TJ, Kuiper J. Oxidized low-density lipoprotein as a delivery system for photosensitizers: implications for photodynamic therapy of atherosclerosis. *J Pharmacol Exp Ther*. 1999;289(1):528–534.
93. Lin JS, Wang CJ, Li WT. Photodynamic therapy of balloon-injured rat carotid arteries using indocyanine green. *Lasers Med Sci*. 2018;33(5):1123–1130. doi:10.1007/s10103-018-2488-7
94. Yasunaka Y, Aizawa K, Asahara T, Kato H, Hayata Y, Ishikura IA. In vivo accumulation of photosensitizers in atherosclerotic lesions and blood in atherosclerotic rabbit. *Lasers Life Sci*. 1991;1991:53–65.
95. Hayashi J, Saito T, Aizawa K. Photodynamic diagnosis and treatment for atherosclerosis by an endoscopic approach. *Diagn Ther Endosc*. 1999;5(3):191–195. doi:10.1155/DTE.5.191
96. Hamblin MR, Miller JL, Ortel B. Scavenger-receptor targeted photodynamic therapy. *Photochem Photobiol*. 2000;72(4):533–540. doi:10.1562/0031-8655(2000)072<0533:SRTPT>2.0.CO;2

97. Shon S-M, Choi Y, Kim J-Y, et al. Photodynamic therapy using a protease-mediated theranostic agent reduces cathepsin-B activity in mouse atheromata in vivo. *Arterioscler Thromb Vasc Biol*. 2013;33(6):1360–1365. doi:10.1161/ATVBAHA.113.301290
98. Lee DK, Choi Y, Shon SM, Schellingerhout D, Park JE, Kim DE. Atorvastatin and clopidogrel interfere with photosensitization in vitro. *Photochem Photobiol Sci*. 2011;10(10):1587–1592. doi:10.1039/c0pp00363h
99. Weiss-Sadan T, Ben-Nun Y, Maimoun D, et al. A theranostic cathepsin activity-based probe for noninvasive intervention in cardiovascular diseases. *Theranostics*. 2019;9(20):5731–5738. doi:10.7150/thno.34402
100. Chen Z, Woodburn KW, Shi C, Adelman DC, Rogers C, Simon DI. Photodynamic therapy with motexafin lutetium induces redox-sensitive apoptosis of vascular cells. *Arterioscler Thromb Vasc Biol*. 2001;21(5):759–764. doi:10.1161/01.atv.21.5.759
101. Yamaguchi A, Woodburn KW, Hayase M, Robbins RC. Reduction of vein graft disease using photodynamic therapy with motexafin lutetium in a rodent isograft model. *Circulation*. 2000;102(19 Suppl 3):III275–III280. doi:10.1161/01.cir.102.suppl_3.iii-275
102. Yamaguchi A, Woodburn KW, Hayase M, Hoyt G, Robbins RC. Photodynamic therapy with motexafin lutetium (Lu-Tex) reduces experimental graft coronary artery disease. *Transplantation*. 2001;71(11):1526–1532. doi:10.1097/00007890-200106150-00008
103. Saito T, Hayashi J, Sato H, Kawabe H, Aizawa K. Scanning electron microscopic analysis of acute photodynamic therapy for atherosclerotic plaques of rabbit aorta by using a pheophorbide derivative. *J Clin Laser Med Surg*. 1996;14(1):1–6. doi:10.1089/clm.1996.14.1
104. Huang L, Chen Q, Yu L, Bai D. Pyropheophorbide-alpha methyl ester-mediated photodynamic therapy induces apoptosis and inhibits LPS-induced inflammation in RAW264.7 macrophages. *Photodiagnosis Photodyn Ther*. 2019;25:148–156. doi:10.1016/j.pdpdt.2018.12.002
105. Jain M, Bouilloux J, Borrego I, et al. Cathepsin B-cleavable polymeric photosensitizer prodrug for selective photodynamic therapy: in vitro studies. *Pharmaceuticals*. 2022;15(5):564. doi:10.3390/ph15050564
106. Wang G, Zhu Y, Li K, et al. Curcumin-mediated photodynamic therapy inhibits the phenotypic transformation, migration, and foaming of oxidized low-density lipoprotein-treated vascular smooth muscle cells by promoting autophagy. *J Cardiovasc Pharmacol*. 2021;78(2):308–318. doi:10.1097/FJC.0000000000001069
107. Spyropoulos-Antonakakis N, Sarantopoulou E, Trohopoulos PN, et al. Selective aggregation of PAMAM dendrimer nanocarriers and PAMAM/ZnPc nanodrugs on human atheromatous carotid tissues: a photodynamic therapy for atherosclerosis. *Nanoscale Res Lett*. 2015;10:210.
108. Rodriguez L, Vallecorsa P, Battah S, et al. Aminolevulinic acid dendrimers in photodynamic treatment of cancer and atheromatous disease. *Photochem Photobiol Sci*. 2015;14(9):1617–1627. doi:10.1039/c5pp00126a
109. Cespedes MA, Saenz DA, Calvo GH, et al. Apoptotic cell death induced by dendritic derivatives of aminolevulinic acid in endothelial and foam cells co-cultures. *Photochem Photobiol Sci*. 2021;20(4):489–499. doi:10.1007/s43630-021-00025-x
110. Wennink JWH, Liu Y, Mäkinen PI, et al. Macrophage selective photodynamic therapy by meta-tetra(hydroxyphenyl)chlorin loaded polymeric micelles: a possible treatment for cardiovascular diseases. *Eur J Pharm Sci*. 2017;107:112–125. doi:10.1016/j.ejps.2017.06.038
111. Kim H, Kim Y, Kim IH, Kim K, Choi Y. ROS-responsive activatable photosensitizing agent for imaging and photodynamic therapy of activated macrophages. *Theranostics*. 2013;4(1):1–11. doi:10.7150/thno.7101
112. Song JW, Ahn JW, Lee MW, et al. Targeted theranostic photoactivation on atherosclerosis. *J Nanobiotechnology*. 2021;19(1):338. doi:10.1186/s12951-021-01084-z
113. Ahn JW, Kim JH, Park K. In vitro photodynamic effects of the inclusion nanocomplexes of glucan and chlorin e6 on atherogenic foam cells. *Int J Mol Sci*. 2020;22(1):177. doi:10.3390/ijms22010177
114. Han XB, Li HX, Jiang YQ, et al. Upconversion nanoparticle-mediated photodynamic therapy induces autophagy and cholesterol efflux of macrophage-derived foam cells via ROS generation. *Cell Death Dis*. 2017;8(6):e2864. doi:10.1038/cddis.2017.242
115. Xu M, Mao C, Chen H, et al. Osteopontin targeted theranostic nanoprobes for laser-induced synergistic regression of vulnerable atherosclerotic plaques. *Acta Pharm Sin B*. 2022;12(4):2014–2028. doi:10.1016/j.apsb.2021.12.020
116. Zhu X, Wang H, Zheng L, et al. Upconversion nanoparticle-mediated photodynamic therapy induces THP-1 macrophage apoptosis via ROS bursts and activation of the mitochondrial caspase pathway. *Int J Nanomedicine*. 2015;10:3719–3736. doi:10.2147/IJN.S82162
117. Han X, Kou J, Zheng Y, et al. ROS generated by upconversion nanoparticle-mediated photodynamic therapy induces autophagy via PI3K/AKT/mTOR signaling pathway in M1 peritoneal macrophage. *Cell Physiol Biochem*. 2019;52(6):1325–1338.
118. Ma Y, Ma Y, Gao M, et al. Platelet-Mimicking therapeutic system for noninvasive mitigation of the progression of atherosclerotic plaques. *Adv Sci*. 2021;8(8):2004128. doi:10.1002/advs.202004128
119. Mu D, Wang X, Wang H, et al. Chemiexcited photodynamic therapy integrated in polymeric nanoparticles capable of MRI against atherosclerosis. *Int J Nanomedicine*. 2022;17:2353–2366. doi:10.2147/IJN.S355790
120. Usui M, Miyagi M, Fukasawa S, et al. A first trial in the clinical application of photodynamic therapy for the prevention of restenosis after coronary-stent placement. *Lasers Surg Med*. 2004;34(3):235–241. doi:10.1002/lsm.20018
121. Rockson SG, Kramer P, Razavi M, et al. Photoangioplasty for human peripheral atherosclerosis: results of a Phase I trial of photodynamic therapy with motexafin lutetium (Antrin). *Circulation*. 2000;102(19):2322–2324. doi:10.1161/01.cir.102.19.2322
122. Kereiakes DJ, Szyniszewski AM, Wahr D, et al. Phase I drug and light dose-escalation trial of motexafin lutetium and far red light activation (phototherapy) in subjects with coronary artery disease undergoing percutaneous coronary intervention and stent deployment: procedural and long-term results. *Circulation*. 2003;108(11):1310–1315. doi:10.1161/01.CIR.0000087602.91755.19
123. Choi V, Rajora MA, Zheng G. Activating drugs with sound: mechanisms behind sonodynamic therapy and the role of nanomedicine. *Bioconjug Chem*. 2020;31(4):967–989. doi:10.1021/acs.bioconjchem.0c00029
124. Yumita N, Nishigaki R, Umemura K, Umemura S-I. Hematoporphyrin as a sensitizer of cell-damaging effect of ultrasound. *Jpn J Cancer Chemother*. 1989;80(3):219–222. doi:10.1111/j.1349-7006.1989.tb02295.x
125. Arakawa K, Hagisawa K, Kusano H, et al. Sonodynamic therapy decreased neointimal hyperplasia after stenting in the rabbit iliac artery. *Circulation*. 2002;105(2):149–151. doi:10.1161/hc0202.102921
126. Cao Z, Zhang T, Sun X, et al. Membrane-permeabilized sonodynamic therapy enhances drug delivery into macrophages. *PLoS One*. 2019;14(6):e0217511. doi:10.1371/journal.pone.0217511
127. Cheng J, Sun X, Guo S, et al. Effects of 5-aminolevulinic acid-mediated sonodynamic therapy on macrophages. *Int J Nanomedicine*. 2013;8:669–676. doi:10.2147/IJN.S39844
128. Chen H, Gao W, Yang Y, et al. Inhibition of VDAC1 prevents Ca^{2+}-mediated oxidative stress and apoptosis induced by 5-aminolevulinic acid mediated sonodynamic therapy in THP-1 macrophages. *Apoptosis*. 2014;19(12):1712–1726. doi:10.1007/s10495-014-1045-5

129. Wang H, Yang Y, Chen H, et al. The predominant pathway of apoptosis in THP-1 macrophage-derived foam cells induced by 5-aminolevulinic acid-mediated sonodynamic therapy is the mitochondria-caspase pathway despite the participation of endoplasmic reticulum stress. *Cell Physiol Biochem*. 2014;33(6):1789–1801. doi:10.1159/000362958
130. Sun X, Guo S, Wang W, et al. Potential involvement of the 18 kDa translocator protein and reactive oxygen species in apoptosis of THP-1 macrophages induced by sonodynamic therapy. *PLoS One*. 2018;13(5):e0196541. doi:10.1371/journal.pone.0196541
131. Wang H, Yang Y, Sun X, et al. Sonodynamic therapy-induced foam cells apoptosis activates the phagocytic PPARγ-LXRα-ABCA1/ABCG1 pathway and promotes cholesterol efflux in advanced plaque. *Theranostics*. 2018;8(18):4969–4984. doi:10.7150/thno.26193
132. Yang Y, Wang J, Guo S, et al. Non-lethal sonodynamic therapy facilitates the M1-to-M2 transition in advanced atherosclerotic plaques via activating the ROS-AMPK-mTORC1-autophagy pathway. *Redox Biol*. 2020;32:101501. doi:10.1016/j.redox.2020.101501
133. Wang Y, Wang W, Xu H, et al. Non-lethal sonodynamic therapy inhibits atherosclerotic plaque progression in ApoE-/- mice and attenuates ox-LDL-mediated macrophage impairment by inducing heme oxygenase-1. *Cell Physiol Biochem*. 2017;41(6):2432–2446. doi:10.1159/000475913
134. Li Z, Sun X, Guo S, et al. Rapid stabilisation of atherosclerotic plaque with 5-aminolevulinic acid-mediated sonodynamic therapy. *Thromb Haemost*. 2015;114(4):793–803. doi:10.1160/TH14-12-1030
135. Sun X, Guo S, Yao J, et al. Rapid inhibition of atherosclerotic plaque progression by sonodynamic therapy. *Cardiovasc Res*. 2019;115(1):190–203. doi:10.1093/cvr/cvy139
136. Li B, Gong J, Sheng S, et al. Sonodynamic therapy reduces iron retention of hemorrhagic plaque. *Bioeng Transl Med*. 2021;6(1):e10193. doi:10.1002/btm2.10193
137. Cao Y, Yao J, Gao W, et al. Sonodynamic therapy promotes efferocytosis via CD47 down-regulation in advanced atherosclerotic plaque. *Int Heart J*. 2022;63(1):131–140. doi:10.1536/ihj.21-233
138. Yao J, Gao W, Wang Y, et al. Sonodynamic therapy suppresses neovascularization in atherosclerotic plaques via macrophage apoptosis-induced endothelial cell apoptosis. *JACC*. 2020;5(1):53–65. doi:10.1016/j.jacbts.2019.10.007
139. Gao Q, Wang F, Guo S, et al. Sonodynamic effect of an anti-inflammatory agent–emodin on macrophages. *Ultrasound Med Biol*. 2011;37(9):1478–1485. doi:10.1016/j.ultrasmedbio.2011.05.846
140. Wang F, Gao Q, Guo S, et al. The sonodynamic effect of curcumin on THP-1 cell-derived macrophages. *Biomed Res Int*. 2013;2013:737264. doi:10.1155/2013/737264
141. Zheng L, Sun X, Zhu X, et al. Apoptosis of THP-1 derived macrophages induced by sonodynamic therapy using a new sonosensitizer hydroxyl acetylated curcumin. *PLoS One*. 2014;9(3):e93133. doi:10.1371/journal.pone.0093133
142. Zheng L, Li Y, Li X, et al. Combination of Hydroxyl Acetylated Curcumin and Ultrasound Induces Macrophage Autophagy with Anti-Apoptotic and Anti-Lipid Aggregation Effects. *Cell Physiol Biochem*. 2016;39(5):1746–1760. doi:10.1159/000447875
143. Jiang Y, Kou J, Han X, et al. ROS-Dependent Activation of Autophagy through the PI3K/Akt/mTOR Pathway Is Induced by Hydroxysafflor Yellow A-Sonodynamic Therapy in THP-1 Macrophages. *Oxid Med Cell Longev*. 2017;2017:8519169. doi:10.1155/2017/8519169
144. Kou JY, Li Y, Zhong ZY, et al. Berberine-sonodynamic therapy induces autophagy and lipid unloading in macrophage. *Cell Death Dis*. 2017;8(1):e2558. doi:10.1038/cddis.2016.354
145. Li X, Gao L, Zheng L, et al. The efficacy and mechanism of apoptosis induction by hypericin-mediated sonodynamic therapy in THP-1 macrophages. *Int J Nanomedicine*. 2015;10:821–838. doi:10.2147/IJN.S75398
146. Zheng X, Wu J, Shao Q, et al. Apoptosis of THP-1 macrophages induced by pseudohypericin-mediated sonodynamic therapy through the mitochondria-caspase pathway. *Cell Physiol Biochem*. 2016;38(2):545–557. doi:10.1159/000438649
147. Li X, Zhang X, Zheng L, et al. Hypericin-mediated sonodynamic therapy induces autophagy and decreases lipids in THP-1 macrophage by promoting ROS-dependent nuclear translocation of TFEB. *Cell Death Dis*. 2016;7(12):e2527. doi:10.1038/cddis.2016.433
148. Goncalves KD, Vieira DP, Courrol LC. Synthesis and characterization of aminolevulinic acid gold nanoparticles: photo and sonosensitizer agent for atherosclerosis. *J Lumines*. 2018;197:317–323. doi:10.1016/j.jlumin.2018.01.057
149. Gonçalvez KDO, Vieira DP, Courrol LC. Study of THP-1 macrophage viability after sonodynamic therapy using methyl ester of 5-aminolevulinic acid gold nanoparticles. *Ultrasound Med Biol*. 2018;44(9):2009–2017. doi:10.1016/j.ultrasmedbio.2018.05.012
150. Jiang L, Wang J, Jiang J, et al. Sonodynamic therapy in atherosclerosis by curcumin nanosuspensions: preparation design, efficacy evaluation, and mechanisms analysis. *Eur J Pharm Biopharm*. 2020;146:101–110. doi:10.1016/j.ejpb.2019.12.005
151. Yao J, Yang Z, Huang L, et al. Low-Intensity focused ultrasound-responsive ferrite-encapsulated nanoparticles for atherosclerotic plaque neovascularization theranostics. *Adv Sci*. 2021;8(19):e2100850. doi:10.1002/advs.202100850
152. Jiang Y, Fan J, Li Y, et al. Rapid reduction in plaque inflammation by sonodynamic therapy inpatients with symptomatic femoropopliteal peripheral artery disease:A randomized controlled trial. *Int J Cardiol*. 2021;325:132–139. doi:10.1016/j.ijcard.2020.09.035
153. Cao Y. Nutrient molecule Corona: an update for nanomaterial-food component interactions. *Toxicology*. 2022;476:153253. doi:10.1016/j.tox.2022.153253